AMRA CR 67-09(F)

AMRA CR 67-09(F)

# ANALYSIS AND REVIEW OF MECHANICAL TESTING PROCEDURES FOR BRITTLE MATERIALS



Final Report
March 1967 to February 1968

by

S. A. Bortz
K. T. Burton

July 1968

IIT Research Institute
Chicago, Illinois

Contract DA-19-066-AMC-321(X)



**ARMY MATERIALS AND MECHANICS RESEARCH CENTER**
**WATERTOWN, MASSACHUSETTS 02172**

Mention of any trade names or manufacturers in this report shall not be construed as advertising nor as an official indorsement or approval of such products or companies by the United States Government.

The findings in this report are not to be construed as an official Department of the Army position, unless so designated by other authorized documents.

DISPOSITION INSTRUCTIONS

Destroy this report when it is no longer needed.
Do not return it to the originator.

# ANALYSIS AND REVIEW OF MECHANICAL TESTING PROCEDURES FOR BRITTLE MATERIALS

AMRA CR 67-09(F)
Final Report
March 1967 to February 1968

by
S. A. Bortz
K. T. Burton

July 1968
IIT Research Institute
Chicago, Illinois

Contract DA-19-066-AMC-321(X)
D/A Project 1C024401A330
AMCMS Code 5025.11.296
Ceramic Materials Research for Army Material



ARMY MATERIALS AND MECHANICS RESEARCH CENTER
Watertown, Massachusetts 02172

# ANALYSIS AND REVIEW OF MECHANICAL TESTING PROCEDURES FOR BRITTLE MATERIALS

AMRA CR 67-09(F)
Final Report
March 1967 to February 1968

by
S. A. Bortz
K. T. Burton

July 1968
IIT Research Institute
Chicago, Illinois

Contract DA-19-066-AMC-321(X)
D/A Project 1C024401A330
AMCMS Code 5025.11.296
Ceramic Materials Research for Army Material



ARMY MATERIALS AND MECHANICS RESEARCH CENTER
Watertown, Massachusetts 02172

CONTENTS

CONTENTS (Cont'd)

ILLUSTRATIONS

ILLUSTRATIONS (Cont'd)

TABLES

# FOREWORD

This work was performed by IIT Research Institute, Chicago, Illinois, under AMMRC Contract No. DA-19-066-AMC-321(X) entitled, "Analysis and Review of Mechanical Testing Procedures for Brittle Materials." This contract has been administered by the Army Materials and Mechanics Research Center, Watertown, Massachusetts, with Samuel J. Acquaviva as Project Engineer.

This report covers the period from 16 March 1967 to 15 February 1968.

Work on this contract has been under the direction of S. A. Bortz, Senior Research Engineer, Ceramics Research Division, IITRI. Personnel active in this program were: T. B. Wade, Assistant Engineer, K. T. Burton, Associate Engineer, E. Mazanek and C. Levesque, Technicians.

# ANALYSIS AND REVIEW OF MECHANICAL TESTING PROCEDURES FOR BRITTLE MATERIALS

## I. INTRODUCTION

During the first year of this investigation emphasis was placed on studying test procedures for evaluating elastic properties including tensile, compressive, flexural and torsional strength of brittle materials. These procedures were limited to methods of loading that produce essentially simple uniaxial stress distributions. However, for designers to make the fullest possible use of brittle materials, a more complete knowledge of their properties and an understanding of their failure mechanisms must be available. To predict the behavior of a brittle material under service conditions the designer must know how the material will react under complex stress states. This knowledge can only be obtained from tests developed specifically to study these properties.

Materials used in engineering applications are often loaded in ways that produce complex stress distributions. These include multiaxial stress states, impact, fatigue, and energy of crack propagation. The effect of these phenomena on the behavior of brittle materials is interesting, unexpected, and can be undesirable.

This report includes a discussion of material behavior, test techniques and analytical methods, correlation of laboratory tests and recommended procedures as well as tabular and graphical presentation of test data.

## II. THE NATURE AND PROPERTIES OF MATERIALS

The deformation of materials can be considered on at least three levels of the division of matter. At the atomic and molecular levels, strength is associated with the individual elemental forms of matter held together by electronic forces, but these forces are reduced because of defects and imperfections in the lattice structure. At the macroscopic or phenomenological level, which is the level of practical interest to the design engineer, the material structure is held together by a combination of forces created by defects and the electronic forces. Theoretically, the strength of a material should be reflected by the forces at the atomic level. However, because of the defects in the structure, the useful strength of materials is several orders of magnitude less than that predicted by theoretical analysis. Hence, the fracture strength of brittle materials can best be established through a study of the energy for crack initiation and propagation, static and dynamic fatigue, and a knowledge of fracture toughness which can be accomplished through impact testing and the effect of biaxial stresses. Only when the boundary conditions under which fracture takes place are known, is it possible to consider procedures for testing and designing against its occurrence.

### A. Mechanics of Fracture

One of the principal aims of theories on the behavior of materials is to relate the observable effect of the imposed conditions to the response of the material on a molecular or atomic level or, conversely, to predict the microscopic material properties from the known structure. In the case of ultimate mechanical strength, it would appear that this property should be related to the cohesive forces acting between the elemental particles and their arrangement in the body. The fracture of the material under stress involves the rupture of those bonds which intersect the plane defined by the growing fracture surfaces.

Cleavage fractures occur when a cleavage crack spreads through a solid under a tensile component of the externally applied stress. The material fractures because the concentrated tensile stresses at the crack tip are able to break atomic bonds. Under uniaxial tensile loading the crack tends to propagate perpendicular to the tensile axis. When viewed in profile, cleavage fractures appear 'flat' or 'square'. Since most structural materials are polycrystalline the orientation of the cleavage plane in each grain of the material is usually not perpendicular to the applied stress so that on a microscopic scale, the fractures are not completely flat over distances larger than the grain size. In brittle materials cleavage fractures can propagate continuously from one grain to the next (Figure 1).

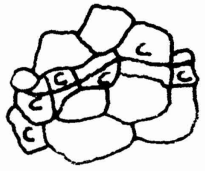


(a) Continuous Cleavage, all grains cleave, C

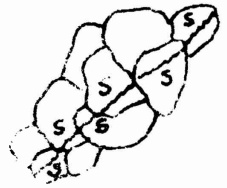


(c) Shear or Shear Rupture


(b) Discontinuous Cleavage, some grains cleave, C others fail in shear, S

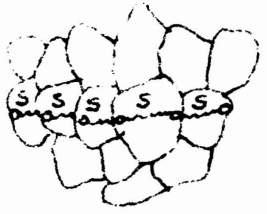


(d) Normal Rupture, results from formation of voids, O, and shear between them

Figure 1. FRACTURE VIEWED AT MICROSCOPIC LEVEL IN TERMS OF PASSAGE OF VARIOUS TYPES OF CRACKS

Shear fracture, which occurs by the shearing of atomic bonds, is actually a process of extremely localized (inhomogeneous) plastic deformation. In crystalline solids, plastic deformation tends to be confined to crystallographic planes of atoms which have a low resistance to shear, shear planes. Shear fracture in a pure single crystal occurs when two halves of the crystal slip apart on the crystallographic glide plane that has the largest amount of shear stress resolved across it. When shear occurs on only one set of parallel planes, a slant fracture is formed; when it takes place in two directions a chisel point fracture occurs. In polycrystalline materials the advancing shear crack tends to follow the path of maximum resolved shear stress. This path is determined by both the applied stress system and the internal plane of weakest resistance due to stress concentrators such as voids and inclusions. Crack growth takes place by the formation of voids and their subsequent coalescence by local plastic strains. The macroscopic fracture path is perpendicular to the tensile axis. On a microscopic scale the fracture is quite jagged, since the crack advances by void coalescence on alternating planes inclined at 30° to 45° to the tensile axis.

Under certain conditions the boundary between grains is weaker than the fracture planes within the grains themselves. In this case fracture then occurs intergranularly by one of the aforementioned processes, rather than through the grains; a phenomena which is termed transgranular fracture.

Fracture takes place by that mode which requires the least amount of local strain at the tip of the advancing crack. At an atomistic level the fracture strength of a material will depend on the strength of its atomic bonds. To estimate this bond strength, let $a_o$ be the equilibrium spacing between atomic planes in the absence of applied stress. The stress ($\sigma$) required to separate the planes to a distance $a > a_o$ increases until the theoretical strength $\sigma_c$ is reached (Figure 2) and the bonds are broken. Further displacement of the atoms can then occur under a reduced applied stress. This stress-displacement curve can be approximated by a sine curve having a wavelength ($\lambda$);

$$\sigma = \sigma_c \sin \left(\frac{2\pi x}{\lambda}\right) \tag{1}$$

where $x = (a - a_o)$ is the displacement from equilibrium. For small displacements the small angle approximation ($\sin x \cong x$) holds; so,

$$\sigma \cong \sigma_c \left(\frac{2\pi x}{\lambda}\right) \tag{2}$$

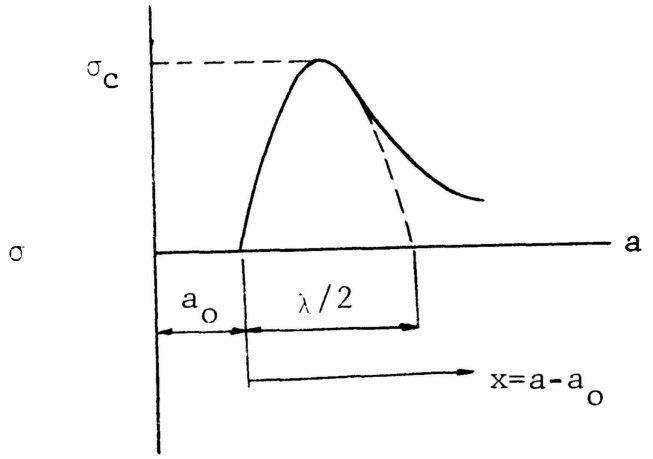


Figure 2. TENSILE STRESS REQUIRED TO SEPARATE ATOMIC PLANES TO A DISTANCE $a>a_o$; $a_o$ IS EQUILIBRIUM SEPARATION AT $\sigma=0$. FRACTURE OCCURS WHEN $\sigma=\sigma_c$.

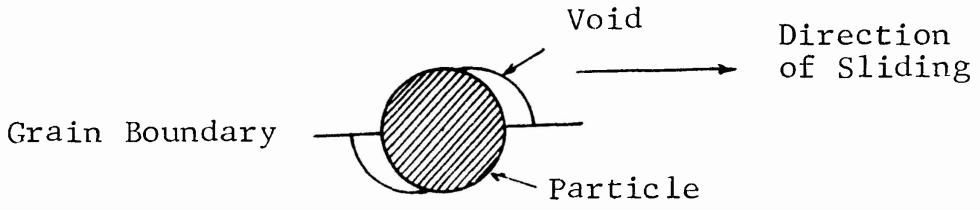


Figure 3. NUCLEATION OF A VOID AT A PARTICLE BY GRAIN BOUNDARY SLIDING

Assuming that these small displacements also obey Hooke's law,

$$\sigma = E\varepsilon = \frac{Ex}{a_o} \tag{3}$$

$$\sigma_c = \frac{\lambda}{2\pi} \frac{E_o}{a_o} \tag{4}$$

where E and $\varepsilon$ are material elastic modulus and material strain, respectively.

For purposes of describing the energy relations during fracture a quantity called true surface energy ($\gamma_s$) can be defined as the work done in creating a new surface area by the breaking of atomic bonds. From Figure 2 this is simply one-half the area under the stress displacement curve since two new surfaces are created each time a bond is broken;

$$2\gamma_s = \int_o^{N2} \sigma_c \sin\left(\frac{2\pi x}{\lambda}\right) dx = \frac{\lambda \sigma_c}{\pi}$$

$$\sigma_c = \sqrt{\frac{E\gamma_s}{a_o}} \tag{5}$$

If a tensile stress is applied perpendicular to an elliptical void of length 2c and height 2h ($2c >> 2h$) the maximum tensile stress, $\sigma(\max)$ occurs at the end of the crack and can be expressed by;

$$\sigma^{(\max)} = \sigma \left(1 + \frac{2c}{h}\right)$$

This stress can be expressed in terms of radius of curvature ($\rho$) at the end of the crack and the nominal stress ($\sigma$). For an ellipse;

$$\rho = h^2/c$$

$$\sigma^{(\max)} = \sigma \left(1 + 2\sqrt{\frac{c}{\rho}}\right)$$

$$\cong 2\sigma \sqrt{\frac{c}{\rho}} \tag{6}$$

A necessary condition for the propagation of an elastic crack is that the maximum tensile stress level at its tip reach the theoretical cohesive stress ($\sigma_c$):

$$2\sigma\sqrt{\frac{c}{\rho}} = \sqrt{\frac{E\gamma_s}{a_o}}$$

$$\sigma = \sqrt{\frac{2E\gamma_s}{\pi c}\left(\frac{\pi\rho}{Ba_o}\right)}$$

$$\cong \sqrt{\frac{2E\gamma_s}{\pi c}\left(\frac{\rho}{3a_o}\right)} \qquad (7)$$

This relation only applies for completely brittle and elastic solids.

Griffith[1] on the basis of thermodynamic considerations derived an equation of similar form;

$$\sigma = \sqrt{\frac{2E\gamma}{\pi c}} \qquad (8)$$

Comparing Eq. 8 with Eq. 7 indicates that $\rho = 3a_o$ is a lower limit of the effective radius of an elastic crack. Cottrell[2] has shown that irrespective of a crack sharpness, some surface energy must be created at the tip of the crack so that $\sigma$ cannot approach zero as $\rho$ approaches zero. Thus when $\rho < 3a_o$, the stress for unstable crack propagation is given by Eq. 8 and when $\rho > 3a_o$ Eq. 7 is used. Both equations must be satisfied if unstable fracture is to occur and local conditions permit the breaking of atomic bonds, thereby reducing the overall free energy of the system. This point is important when plastic deformation accompanies cleavage crack propagation.

The Irwin[3] analysis of fracture proposes that crack propagation occurs at $\sigma$ when a parameter defined as the crack extension force,

$$G = K^2/E \qquad (9)$$

is equal to a critical value, $G_c$, the critical strain energy release rate for unstable crack extension which may be related to fracture toughness. The term G is the material shear modulus and K is called the fracture toughness. For the elastic crack in an infinitely wide plate;

$$\frac{\sigma^2 \pi c}{E} = G_c$$

$$\sigma = \sqrt{\frac{EG}{\pi c}} \qquad (10)$$

A comparison of Eq. 10 and Eq. 8 indicates that,

$$G_c = 2\gamma_s$$

so that the two approaches provide the same result.

This discussion has provided the background for the need of appropriate tests to provide a reliable measure of surface energy and how it can help solve specific questions with regard to fracture propagation and fracture toughness of brittle materials.

B. Resistance to Fracture

Fracturing can be preceded by a large, small, or even negligible amount of permanent deformation. As long as it is certain that a structural member will distort excessively before breaking, there may be no concern with its fracturing characteristics because failure in service will be by yielding. If, on the other hand, the structure breaks after a slight amount of deformation, fracture behavior becomes all important. Since brittle materials usually fall into this latter group, tests which measure fracture resistance are of prime concern to users of brittle materials. Some materials may be classed as ductile under some conditions and brittle in others. The property of particular interest in these materials is toughness. This term may be defined as the amount of energy that is irreversibly absorbed in the process of fracture.

Such a property has little meaning for brittle materials at or near room temperature, but may be of significance in understanding the transition properties of ceramic materials at high temperatures, since toughness of a material is considered as its ability to absorb energy during plastic deformation. In static tensile tests this energy is represented by the area under the tensile test diagram. Brittle materials at ambient temperatures have low toughness since they display little plastic deformation before fracture.

The same material at elevated temperatures may behave as a brittle or a plastic material depending on external conditions. A tensile test of a single crystal of rock salt results in a brittle fracture along one of the principal crystallographic planes if tested at room temperature. The same specimen, if tested in hot water, deforms plastically by sliding along octahedral planes. Similar deformation may occur at higher temperatures for other ceramics.

The fundamental ideas regarding the critical temperature at which the transition from brittle to plastic fracture occurs were enlarged by Davidenkov,[4] and applied to crystalline materials. He was able to predict the influence of various factors

on the value of the critical temperature and show that the predictions were in satisfactory agreement with the experimental facts.

For determining the critical temperature, impact tests were used. Since in the case of brittle fracture the work required to produce failure is many times smaller than that required for plastic fracture, the tests showed a sharp change in the amount of energy absorbed at the critical temperature. Determination of the critical temperature is important if the material is to operate in this environment. This is not normally considered for brittle ceramics; however, for some applications the structure will be operating mostly in this range. Then it is only necessary to employ brittle fracture concepts to design the structure so that it will be strong enough to reach operating temperature. Normal ductile considerations can then be used to design for operation beyond the critical temperature range.

Impact tests are generally performed by rapidly loading either a cantilever or a simply supported beam specimen. However, for brittle materials where energy and adsorption is small, it is likely to be overshadowed by the kinetic energy imparted to the specimen and component parts of the testing machine. One method of overcoming this fault is to use a dropping weight method in which a freely falling body is released from a measured height so that it strikes a specimen with a known velocity and energy. Systems of both types require analysis so that designers may make knowledgable use of this information.

There are three fundamental difficulties that arise in connection with the impact energy values obtained from all groups of materials:

1. The impact value does not readily fit into the scheme of materials testing in which conclusions are drawn from stress-strain curves rather than the area under the curve. Normal material testing differentiates clearly between elastic and plastic deformation whereas the energy measured in an impact test produces both elastic and plastic deformation.

2. The "toughness" of a material is often taken as a fixed mechanical characteristic of a material.

3. There is no generally accepted definition of toughness.

## C. Fracture Under Static Loading

In dealing with the fracture mechanism of brittle materials, the assumption is always made that they contain flaws that serve as stress concentrators. When a load is maintained on a brittle material certain near critical flaws can grow relatively slow and stable until they reach the size of Griffith cracks and

then fracture occurs catastrophically. This time dependent fracturing is termed "delayed fracture" or "static fatigue," and is usually associated with intergranular fracture.

There are two types of voids which can form and grow under static loading conditions; 1) the type found to occur at grain boundary junctions (triple point); and 2) the type found to occur along grain boundaries and can be associated with precipitated impurity particles and vacancy condensation at the grain boundaries under stress. In order for the first type or wedge-type crack to be nucleated, it is necessary that the local stress level exceed the cohesive stress. This is generally caused by grain boundary sliding. This phenomena can be reduced by precipitation of hard particles at the grain boundary to reduce sliding. The effect of grain size on void formation is not straightforward. Grain boundary sliding appears to be greater for small particle sizes than large so that void formation should be greater for the small particle materials. For brittle materials at low temperatures wedge-type cracks probably grow and cause failure by a Griffith type fracture mechanism.

As in the case of wedge-type fractures, grain boundary sliding is a pre-requisite for the second type of static fatigue or cavitation fracture. Most evidence indicates that an impurity phase at the grain boundary is required in the nucleation process (Figure 3). The ease with which a cavity can be nucleated by a sliding process will depend on the binding of the particle to the matrix. As with wedge-type cavities, the void nucleation process becomes easier as the degree of wetting between the impurity and grain decreases. For the void to grow simply by vacancy condensation, the work done must exceed the increase in surface energy caused by the removal from a void of radius r and surface energy $\gamma_s$. The condition for void growth is:

$$\sigma \geq \frac{2\gamma_s}{r} \tag{11}$$

For values of $\sigma$ less than the critical value, the void will disappear by sintering at high temperature. For values of $\sigma$ in excess of the critical, the void will grow in size. Growth by this mechanism is interesting in that the Griffith criterion need not be satisfied.(5) The critical importance of this mechanism of cavity growth lies in the fact that if small cavities exist on transverse boundaries, a statically loaded specimen will fail at high temperatures at stress levels below the creep strength of the grains.

In addition to the vacancy flux made of void growth, grain boundary voids can also grow by a continuation of the void nucleation process of grain boundary sliding. Recent studies(6) of rupture under static loading have shown that although reversing from tensile to compressive stress during a test causes voids to

disappear, compression applied orthogonally to the direction of original tension causes them to grow. This observation is consistent only with a grain boundary sliding mechanism of void growth.

D. Fracture Under Cyclic Loading

Fatigue life is not a material property like elastic modulus, which, under normal conditions is a material constant. The endurance limit of a material is influenced by the test used and numerous other variables. Therefore, for any particular material and condition, it is necessary to examine fatigue data with respect to end-use conditions.

There is reason to believe that the existence of cyclic fatigue is a realistic possibility for brittle materials since under cyclic stresses, dislocations move irreversibly, and their multiplication leads to slip band formation and growth resulting in the nucleation and propagation of cracks. This mechanism has indeed been observed in single-crystal magnesia;(7) the experimental results are shown in Figure 4. The slope of the S-N diagram is small, and the loss in strength up to $10^4$ cycles is not more than 15%. This mechanism can be expected to operate in multicrystalline bodies of refractory materials as well.

This phenomenon has also been verified recently by work on graphite(8) at IITRI. This work was performed as a part of a proof-test experiment. Generally, for brittle materials, fatigue testing is synonymous with proof testing of a material. These tests establish safe repeated load levels and the reaction of a material to long term loadings.

It is recognized that fatigue occurs as the result of plastic deformation both in the initiation and propagation of cracks. Up to the terminal fracture, fatigue is a form of ductile (stable) rupture, although often of an extremely localized nature. While fatigue cracks can be initiated in a number of ways, they usually are nucleated at a free surface. Crack initiation in a brittle material can occur in the grain boundaries at a triple point, or at slip bands created during cyclic loading. Each of these effects can lead to the localization of plastic strain by the creation of these discontinuities. In materials whose slip systems are such that cross slip does not occur easily, these surface effects are not developed. The resistance to cyclic stressing of materials that cannot form these surface stress raisers is quite high.

After a crack is initiated at a surface slip band in a single crystal it will continue to advance into the material along the primary slip planes involved in the creation of the slip band before turning into a plane macroscopically at right angles to the principal tensile stress. Crack growth before the transition is called Stage I growth, while that after the transition is

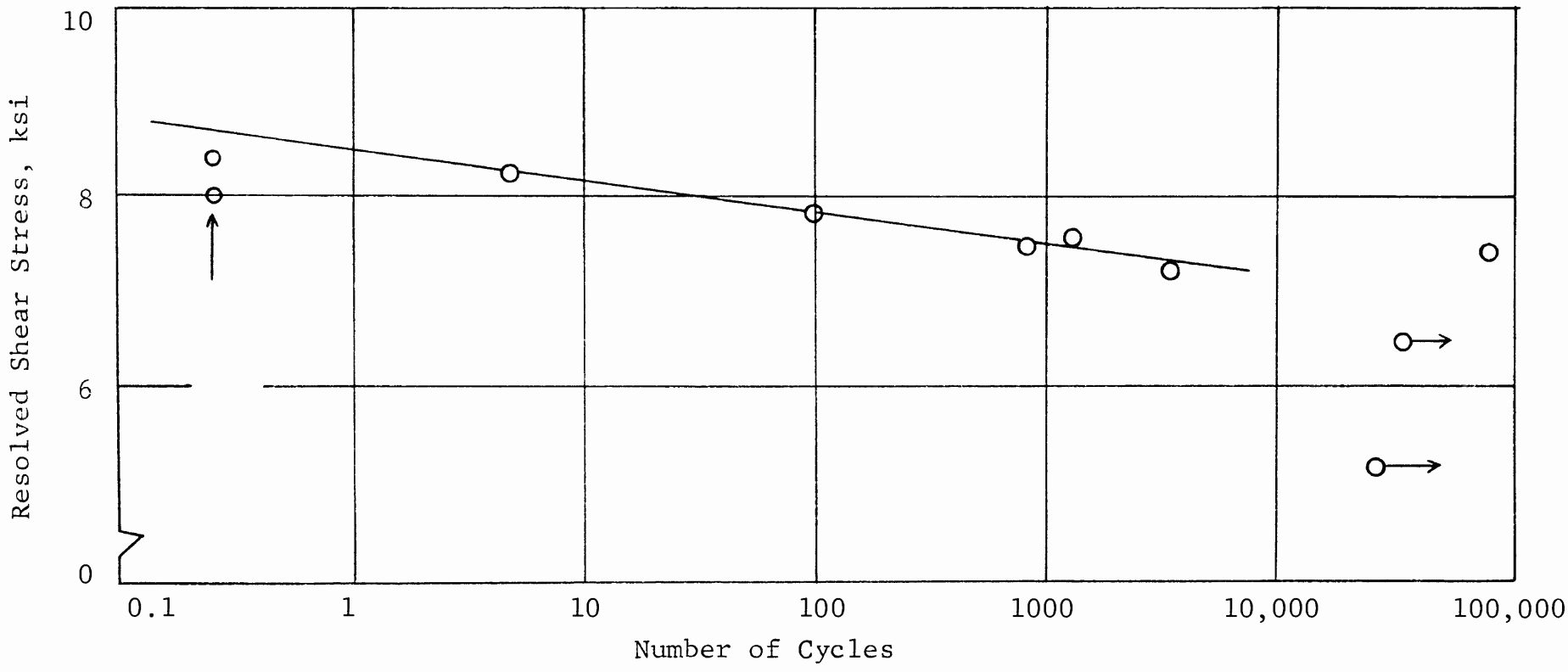


Figure 4. FATIGUE IN MgO SINGLE CRYSTALS

referred to as Stage II growth. The transition is governed by the magnitude of the tensile stress, and the lower the magnitude of this stress, the larger the extent of first stage growth. For this reason Stage I growth is favored in torsion testing, for the tensile component orthogonal to the Stage I crack is low. If the tensile stresses are high enough, Stage I may not occur at all, as in sharply notched specimens; in brittle materials growth occurs entirely in the second mode.

In polycrystalline materials Stage I growth usually terminates when the slip band crack encounters a grain boundary. If the stress amplitude is high enough to nucleate a Stage I crack in a large-grained material, that stress should also be sufficient to cause the crack to propagate through the adjacent grains. In fine-grained materials, cracks may be initiated at a stress that is insufficient for propagation into the adjacent grains. In the one case the failure is due to nucleation of a crack while in the other propagation is the important factor.

Stage II growth can be investigated under conditions of high strain amplitude. As a consequence, the plastic (if any) deformation taking place at the tip of a crack can be observed. One of the important characteristics is that the crack advances a finite increment in each loading cycle. At the start of a loading cycle the crack is sharp, but during extension, as the crack advances, it simultaneously becomes blunter and any plastic zones at the tip expand. It is during the loading stage that a new fracture surface is created. During the unloading portion of the cycle the sharp tip of the crack is re-established. The repetition of this blunting and resharpening process is the basic aspect of Stage II growth. This process continues until the crack becomes long enough to trigger final instability of the crack propagation. In brittle materials the instability criterion is that critical displacement (2c) at which point the crack runs unstably (the Griffith criteria in the elastic range). The two factors that are important in determining the rate of crack growth are the applied stress or strain amplitude and the length of the crack itself, for they determine the stress intensity factor K.

## E. Combined Stresses

The mechanical properties of structural materials are normally determined by tests which subject the specimen to comparatively simple stress conditions. Information concerning the strength of most materials is related to tension or compression, or in some cases, shear. However, the strength of materials under more complicated stress conditions is generally the condition to be met in practice. Data and theories for the behavior of brittle materials, subjected to polyaxial stress states, are important both to the materials scientist and the structural designer. As a matter of fact, it is almost impossible to conceive of an

operational structure in which a simple state of stress can be postulated, much less observed in practice.

In order to determine suitable allowable stresses for complicated stress conditions which occur in practical design, various strength theories have been developed. The purpose of these theories is to predict when failure will occur under combined stresses, assuming that the behavior in a simple tension or compression test is known. The general failure theories, maximum stress, maximum strain, maximum shear, and maximum energy theories, are well documented(9) and will not be discussed in detail. The theory most applicable to brittle materials is the maximum stress law. Salmassy(10) has applied a modified Weibull theory for biaxial stresses and the theoretical curves are shown in Figure 5. The theories predict that tensile strength increases as the compression stress in the normal direction increases; furthermore, the biaxial tensile strength is lower than the uniaxial tensile strength. However, investigators have not provided sufficient experimental results to establish these theories. Griffith has also developed a theory which may apply to brittle materials. The Griffith theory for biaxial stresses follows from the simple Griffith theory for uniaxial stresses. A comparison of the Weibull and Griffith theories and some measured data are shown in Figure 6.

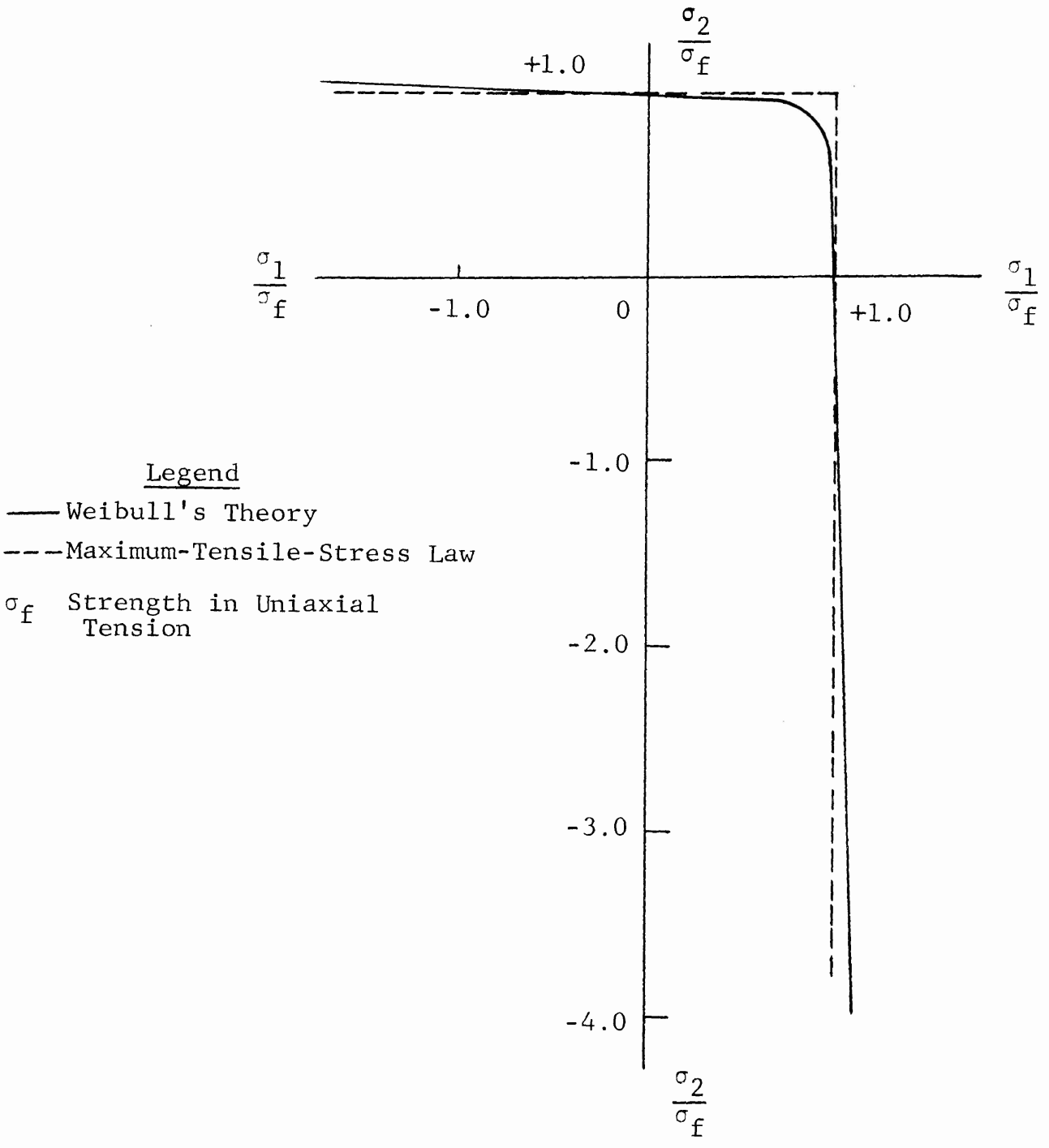


Figure 5. WEIBULL'S THEORY OF STRENGTH FOR BIAXIAL STRESSES FOR HYDROSTONE PLASTER (m=12)

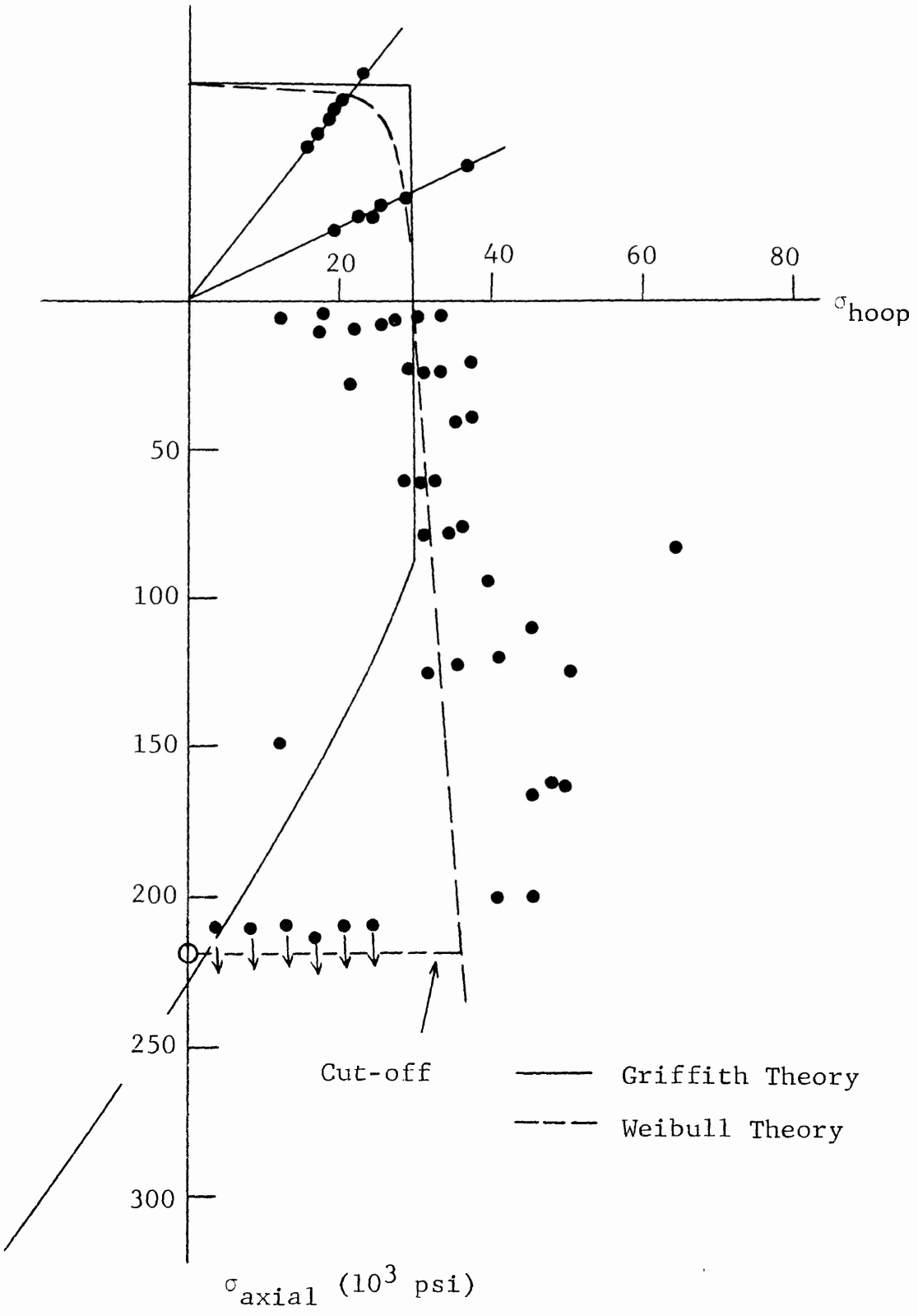


Figure 6. COMPARISON BETWEEN EXPERIMENTAL RESULTS AND THEORY

## III. TEST TECHNIQUES

The previous sections provide a general analysis of the fracture behavior to be expected from brittle materials. The following sections will provide a detailed description and analysis of the test procedures used in studying the fracture behavior and how these various procedures may be inter-related.

### A. Impact Tests

Impact testing is the basis for studying the toughness of materials, that is, the ability of the material to absorb energy during plastic deformation. Brittle materials have low toughness and exhibit only very small plastic deformation before fracture occurs. Failure of such materials takes place suddenly and without forewarning, making their use in structures dangerous unless reliable knowledge of their impact strength is available.

A freely falling body, or a moving load, which strikes a structure delivers an impact, or dynamic load. Problems involving this type of load can be analyzed rather simply on the basis of the following idealized assumptions:

1. Materials behave elastically with no dissipation of energy taking place at the point of impact or at the supports due to local inelastic deformation of the material.

2. The inertia of the system resisting impact can be neglected.

3. The deflection of the system is directly proportional to the applied force whether applied statically or dynamically.

If the principle of conservation of energy is applied, it may also be assumed that at the instant a moving body is stopped, its kinetic energy is transformed entirely into the internal strain energy of the resisting system or fracture of the specimen occurs.

Referring to Figure 7 consider the weight, W, as a freely falling mass striking an elastic system. The static deflection of the spring due to the weight, W, is:

$$\Delta_{stat} = W/k \tag{12}$$

where k = spring constant, lb/in.

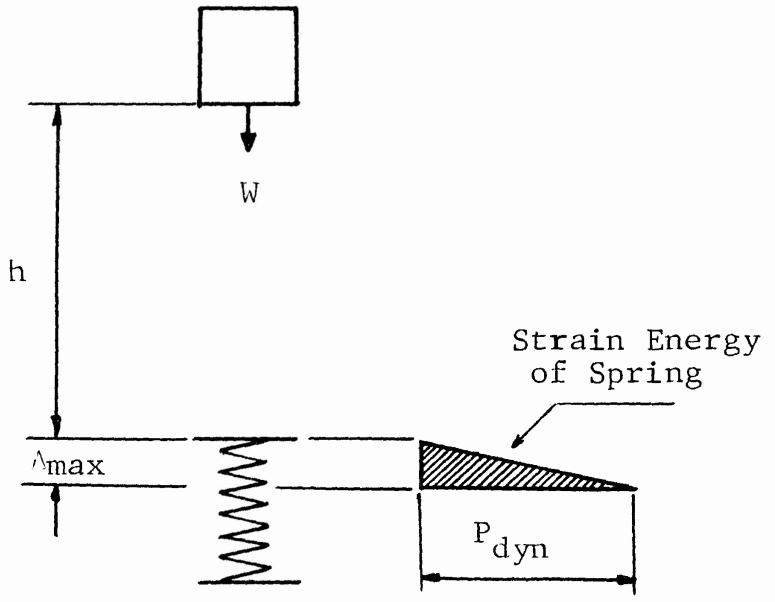


Figure 7. BEHAVIOR OF AN ELASTIC SYSTEM UNDER AN IMPACT FORCE

Similarly, the maximum dynamic deflection is given by:

$$\Delta_{max} = P_{dyn}/k \tag{13}$$

where $P_{dyn}$ = maximum dynamic force exerted on the spring.

Solving for $P_{dyn}$ in terms of the weight, W, and the spring deflection gives:

$$P_{dyn} = \frac{\Delta_{max}}{\Delta_{stat}} \cdot W \tag{14}$$

At the instant the spring deflects its maximum amount, all of the energy of the falling weight is transformed into the energy of the spring. By equating the external work to the internal strain energy, it is seen that:

$$W(h + \Delta_{max}) = \tfrac{1}{2} P_{dyn} \cdot \Delta_{max} \tag{15}$$

By substituting for $P_{dyn}$ in Eq. 14, we have:

$$W(h + \Delta_{max}) = \tfrac{1}{2} \frac{(\Delta_{max})^2}{\Delta_{stat}} \cdot W \tag{16}$$

or,

$$(\Delta_{max})^2 - 2\Delta_{stat}\Delta_{max} - 2h\Delta_{stat} = 0$$

from which:

$$\Delta_{max} = \Delta_{stat}\left(1 + \sqrt{\frac{2h}{\Delta_{stat}}}\right) \tag{17}$$

Again using Eq. 14 it can be shown that:

$$P_{dyn} = W\left(1 + \sqrt{1 + \frac{2h}{\Delta_{stat}}}\right) \tag{18}$$

To apply Eqs. 17 or 18, the static deflection, $\Delta_{stat}$, caused by the gradually applied load, W, can be obtained using any known method. The terms in parentheses of Eqs. 17 and 18 represent the magnification effects of a static force applied dynamically to a system and are called the "impact factor."

Three types of impact tests were conducted in this phase of the program, Izod, Charpy, and Drop Weight.

When a dynamically applied load strikes a test specimen, local damage to the material at the point of impact leads to concentrated stresses which may exceed the nominal stress. The local damage occurs in the form of an indentation and its effect will depend on the notch sensitivity of the material. If the specimen is pre-notched and the dynamic load is applied through the notched cross section, then the notch effect of the striking edge of the applied load is superimposed on the maximum bending stress.

Materials that exhibit plastic deformation are able to reduce the effects of stress concentrations, but brittle materials are unable to do so and the stress concentrations lead to cracks which develop over the whole cross section. In addition, the force of impact and hence the notch effect depend on the section modulus of the specimen. Spath,[11] has shown that, for these reasons, brittle materials exhibit no clear-cut relationship between breaking load and section modulus, so that impact bending stresses cannot be calculated.

However, if the energy absorbed during impact for an un-notched specimen is compared with that absorbed by a pre-notched specimen, then the notch sensitivity ratio can be expressed by:

$$NSR = \frac{K_u}{K_n} \tag{19}$$

where $K_u$ = impact energy of un-notched specimen
$K_n$ = impact energy of pre-notched specimen

Tetelman and McEvily[12] have shown that the NSR is influenced by the flank angle (angle between faces) of a preformed notch, the greater the angle, the lower the NSR. Mild steel specimens with a flank angle of zero (parallel faces) had a notch concentration factor of 2.57, while for a 45° angle notch the factor was 2.18. Brittle materials, would be expected to have greater notch sensitivity factors than these.

1. Izod Impact Test

The Izod impact test measures the energy required to break a vertical cantilever beam specimen. The principle involves striking the specimen with a hammer mounted on the end of a pendulum as shown in Figure 8. The position of the pendulum at the beginning of the swing, together with the weight of the hammer is a measure of the kinetic energy at the point of impact on the specimen. After striking the specimen, the hammer makes contact with an indicator which measures the amount of energy required to break the specimens. The swing of the hammer after impact decreases as the amount of energy required to break the specimen increases.

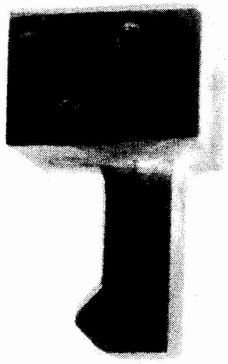

Izod Head

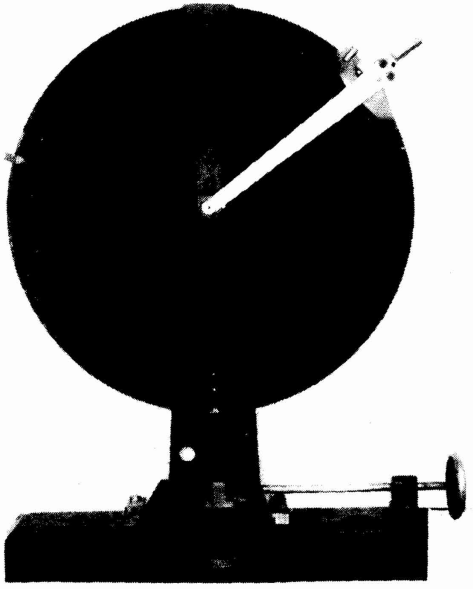

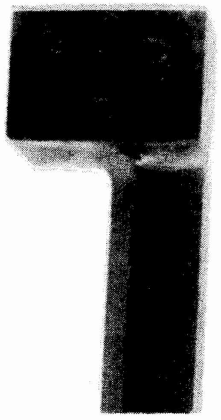

Charpy Head

Figure 8. IMPACT TESTING MACHINE

Before Izod tests are made, calibration of the testing apparatus is essential to determine the loss in kinetic energy due to friction, aerodynamic drag and release mechanism. Calibration of the machine was carried out by making 50 free swings with a standard 50 in.-lb pendulum tester. The calibration procedure showed that the average machine losses were 0.12 in.-lb and the mean energy value of 49.88 in.-lb had a coefficient of variance of only 0.36%. Despite the low resolution, it was believed that machine losses would still be a significant factor in evaluating the impact energy of Poco-Graphite, a low toughness brittle material.

To investigate the possible effects of machine resolution on impact energy a lighter impact pendulum (17.19 in.-lb) having higher resolution was designed for the Izod tests. In this way, the impact energy of the material resulting from tests using a light pendulum with high machine resolution could be compared with that resulting from tests using a heavy pendulum of low resolution. The comparison would be a measure of the significance of machine resolution on impact energy of brittle materials.

The Izod head was calibrated, as before, by making 50 free swings of the pendulum. For this lighter head, the average energy of the testing apparatus was found to be 14.61 in.-lb with a standard deviation of 0.47 in.-lb and a coefficient of variation of 3.24%. Machine resolution was therefore considerably higher with the lighter pendulum than with the standard 50 in.-lb head.

Two types of specimens were used for the Izod tests. Rectangular prisms of Poco-Graphite were cut and machined to $\frac{1}{4} \times \frac{1}{4} \times 3\frac{1}{2}$ in. long (Figure 10). Each specimen was carefully measured to insure that the cross section dimensions fell within the required permitted tolerances of ±0.003 in. One group of specimens were un-notched while the second group contained a V-notch at midspan, 0.05 in. deep. The purpose of the notched specimens was to investigate the effect of stress raisers on the impact energy of the material.

The test procedure involved mounting the specimen in the holding device and allowing the pendulum to fall. After striking the specimen, the pendulum moved the indicator to a position on the calibrated scale from which the impact energy required to break the specimen was recorded. Since the major source of variation in the data obtained from the Izod test is related to the inherent losses in the testing apparatus, it was anticipated that the scatter in the data obtained would be relatively high.

It was determined by test that the resolution of the Izod testing apparatus was dependent upon the kinetic energy of the pendulum. Therefore, these tests were set up for a fixed drop of the Izod head making them destructive tests. As such, the specimens could not be used to evaluate the effects of cumulative

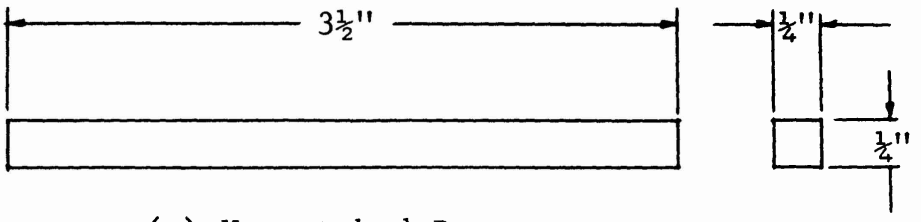


(a) Un-notched Beam

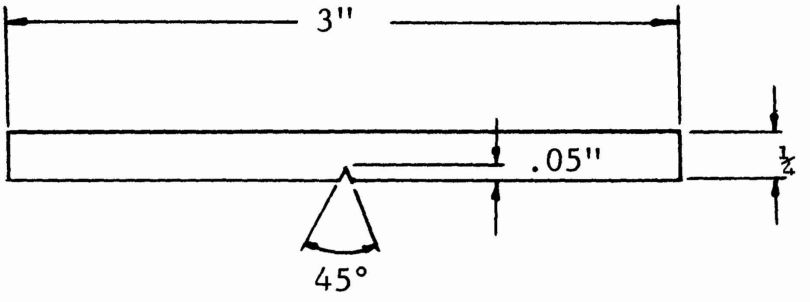


(b) Notched Beam

(c) Photograph of Notched Beam

Figure 10. IMPACT BEAM SPECIMENS

damage to the material resulting from repeated applications of an impact force. In order to observe the phenomena of repeated load applications, a variation in testing technique was pursued. In this phase of the test procedure, the position of the pendulum was lowered so that the available kinetic energy of the hammer was less than the average measured impact energy of the material. The pendulum was released and allowed to strike the specimen once. If the specimen did not break, the pendulum was raised a small increment and again allowed to fall, the process being repeated until the specimen finally fractured. A comparison of the impact force required to produce fracture with the impact energy from the standard Izod tests can then be considered a measure of the cumulative damage due to repeated applications of a dynamically applied load.

2. Charpy Impact Test

The Charpy impact test is similar in nature to the Izod impact test in that it makes use of a hammer mounted in a pendulum. The principal difference between the two forms of impact testing lies in the position of the specimen when it is struck by the hammer. In the Charpy test, the specimen is treated as a simply supported beam as opposed to the vertical cantilever of the Izod test. All of the disadvantages applicable to the Izod test are inherent in the Charpy test since the apparatus used (Figure 8) is the same machine but uses a different type of head for striking the specimen.

As with the Izod test procedure, calibration of the apparatus prior to testing the specimen is necessary to evaluate energy losses due to machine components and aerodynamic drag. The Charpy head for the standard 50 in.-lb pendulum tester is almost the same weight as that of the Izod 50 in.-lb pendulum. It was shown previously that the resolution of the large Izod pendulum was too low for accurate appraisal of the impact energy of Poco-Graphite and on this basis, the 50 in.-lb Charpy pendulum tests were omitted and only the lighter, 18.32 in.-lb pendulum tester was used in the Charpy impact tests. Fifty free swings of the 18.32 in.-lb Charpy head gave an average energy value of 17.23 in.-lb with a standard deviation of only 0.22 in.-lb and a coefficient of 1.29%. Machine losses for the Charpy pendulum were 1.10 in.-lb compared to 2.58 in.-lb for the 17.19 in.-lb Izod pendulum. Machine resolution for the Charpy pendulum was considerably less than for the Izod pendulum, a factor which was anticipated would be reflected in the test results.

Specimens used in the Charpy tests were identical to those used in the Izod tests, and were machined to the same close tolerances. Notched specimens were again used for evaluating the effects of stress raisers on the impact energy of the material. In the Charpy notched impact test, the pendulum head strikes the specimen directly behind the tip of the notch, whereas in the Izod

test, the specimen is struck at a point slightly away from the notch. It is therefore to be expected that the results from the notched impact tests will be influenced by the relationship between the location of the applied force and the point of the notch tip.

Each specimen in the Charpy test procedure is fractured by one swing of the pendulum and again, as with the Izod technique, cumulative damage due to repeated applications of load cannot be evaluated. The technique used to evaluate the effects of cumulative damage to the specimen in the Izod tests were duplicated for these Charpy tests.

3. Drop Weight Test

The drop weight testing technique is relatively new. In essence it is a Charpy type test without the disadvantages of the Charpy test apparatus. As shown in Figure 9, the apparatus consists of a frame which supports an electromagnet. Centered directly under the electromagnet are the supports for a simple beam specimen $\frac{1}{4}$ x $\frac{1}{4}$ x $3\frac{1}{2}$ in. long (Figure 10).

As with the Izod and Charpy techniques, drop weight testing procedure involves releasing a known weight from any given height onto the specimen. Because the equipment for drop weight testing contains no components which create machine losses, no calibration procedure is necessary. The position of the electromagnet can be set at various heights in the frame to establish the upper and lower limits of failure probability for a sample population of the total number of specimens. In this way, a probability of failure curve ranging from 0 to 100% can be drawn.

With the exception of that portion of the curve representing 100% failure of the sample population, specimens not failing at other energy levels can be subjected to repeated applications of impact load to evaluate cumulative damage to the material.

From the preceding description of the impact test techniques followed in this phase of the program, it can be seen that the drop weight method has three distinct advantages over the Izod and Charpy techniques.

First, the apparatus used in drop weight testing is effective yet simple in construction. There are no mechanical parts to contribute to machine losses and hence the calibration procedure necessary for the Izod and Charpy techniques is entirely eliminated. One simple operation of raising or lowering the height of the electromagnet is all that is required to proceed with the actual testing of the specimen.

Second, because of the nature of the testing procedure adopted, the drop weight method is better suited to a "probability

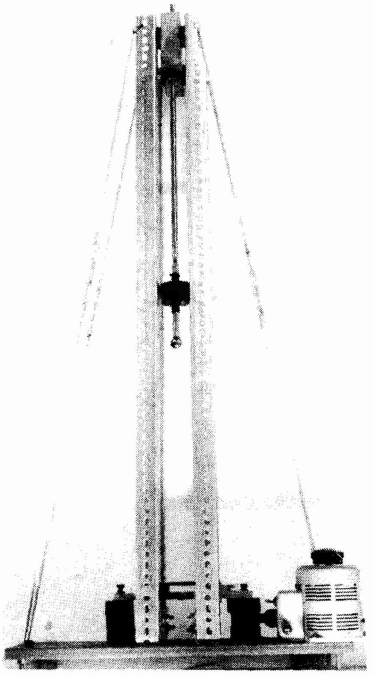

Figure 9. DROP WEIGHT TESTING MACHINE

of failure" type of analysis. The Charpy and Izod tests, conducted in this program for a fixed position of the weighted pendulum lends itself to an "analysis of variance" statistical approach. It is believed that, because of the unpredictable nature of brittle materials with all of the complexities associated with their behavior, the "probability of failure" approach is a more acceptable method to evaluate strength properties.

Third, the theoretical analysis reviewed at the beginning of this section can be applied directly and without modification to the drop weight test technique. Certain factors related to machine losses and aerodynamic drag would have to be introduced in this mathematical procedure before it could be used in connection with the Izod and Charpy tests.

## B. Fatigue Tests

Fatigue strength is the term used to describe the ability of a material to withstand sustained loads over long periods of time or to stand up under the action of repeated applications of loads producing varying stresses. It is well known that under such conditions, materials fail at stresses considerably smaller than the ultimate strength of the material under static loading. Generally, it can be stated that the magnitude of stress required to produce failure decreases as:

1. The length of time over which the load is maintained increases, or

2. The number of cycles of stress increase.

Four types of tests were conducted in this phase of the investigation, two of them directed toward static fatigue behavior and two to cyclic behavior.

### 1. Static Tensile Fatigue

In this type of test, the specimens are loaded in uniaxial tension with dead weights producing a wide range of stress levels maintained for periods of time ranging from 100 to 400 hr. After the specified period of time has elapsed for any given stress level, the loads are removed and the specimen tested to evaluate loss of strength, if any, due to the sustained load.

The specimens used in these tests were of the shape and size shown in Figure 11. The specimen is mounted in the test frame (Figure 12) by an arrangement of pins and grips; a similar arrangement being used to add the dead load to the specimen.

Only one problem is associated with this rather straightforward technique. In the previous report[13] which concerned uniaxial strength tests of Poco-Graphite the problem of alignment

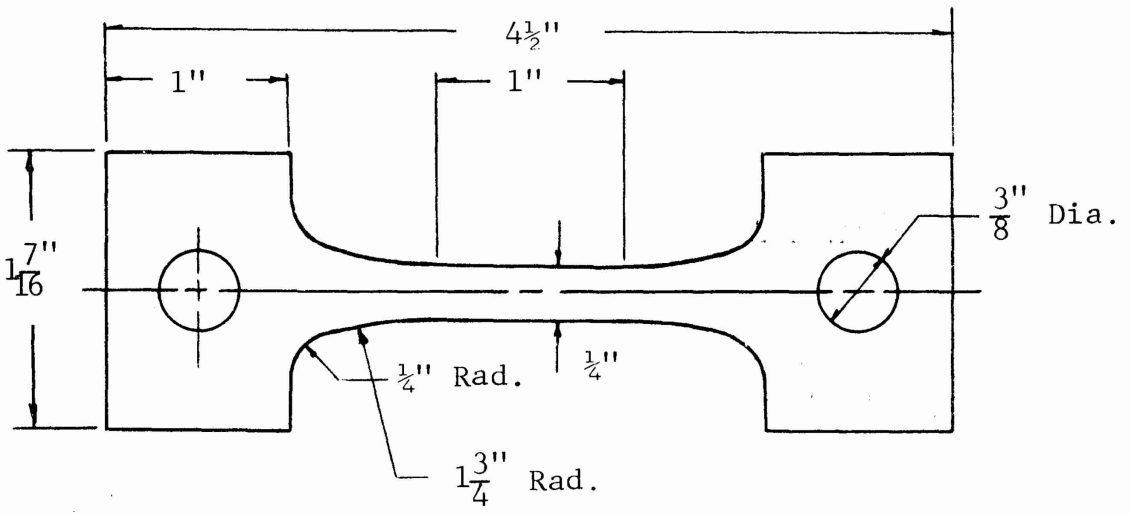


(a) Static Tensile Fatigue Specimen

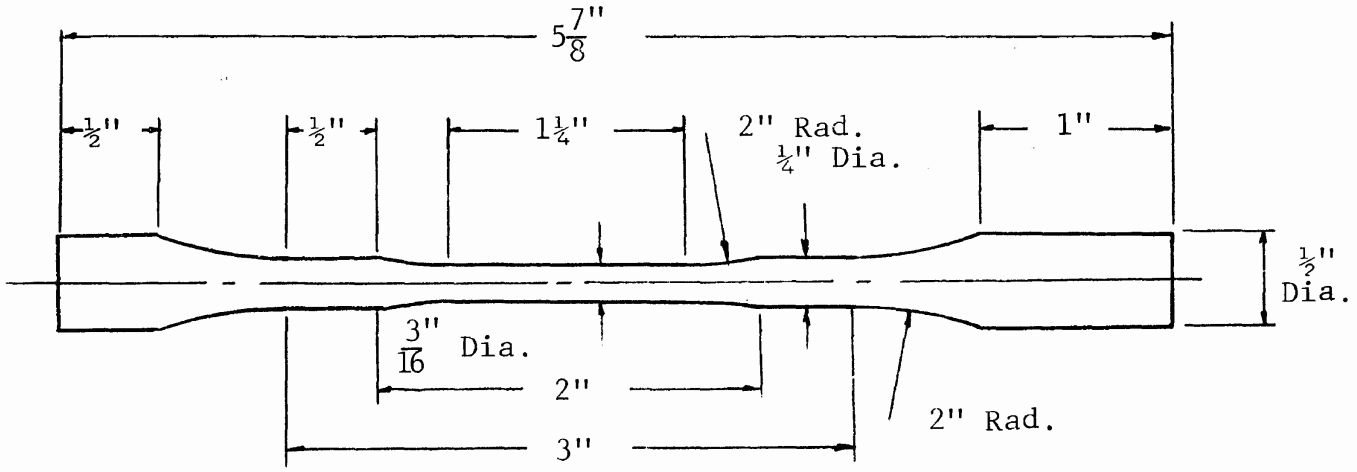


(b) Rotating Beam Fatigue Specimen

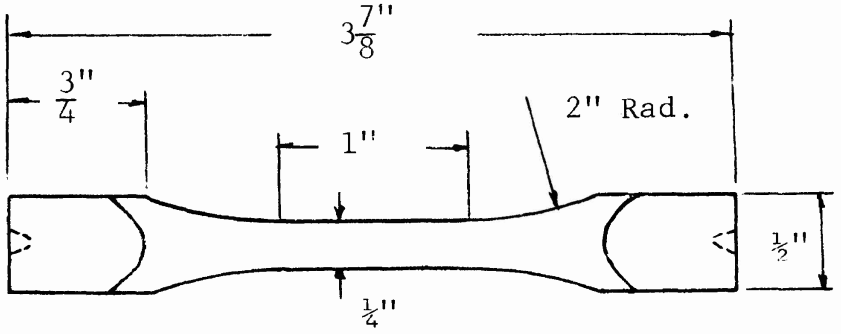


(c) Torsional Fatigue Specimen

Figure 11. FATIGUE SPECIMEN DETAILS

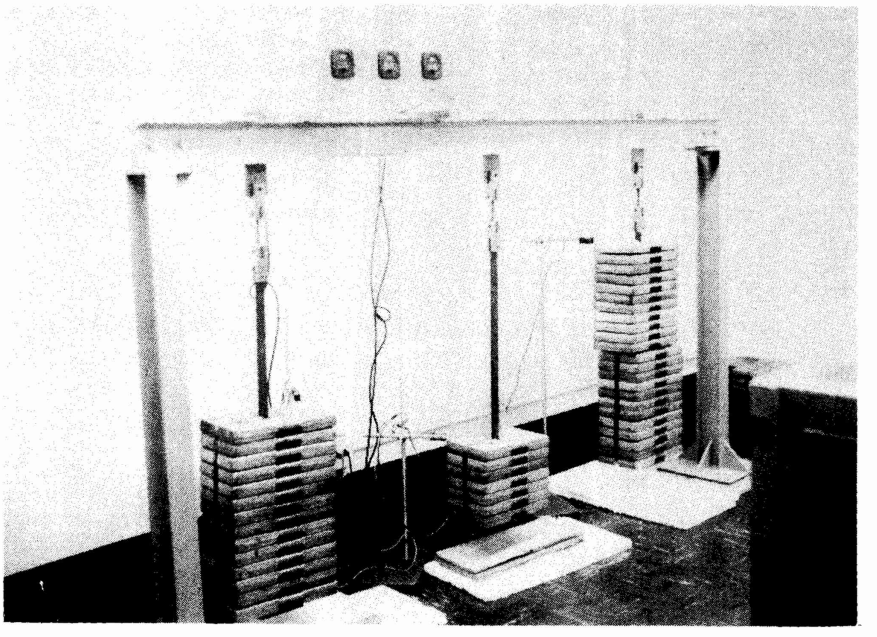

(a) Testing Frame for Sustained Tensile Loads

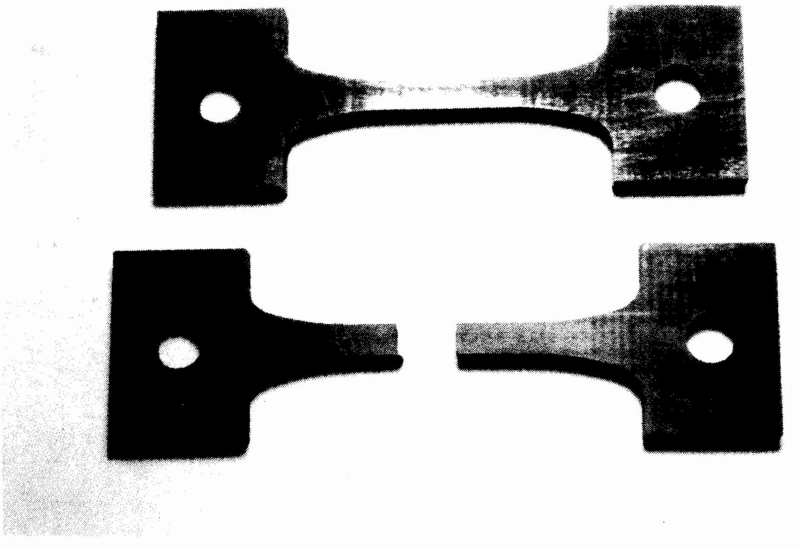

(b) Specimens Before and After Test

Figure 12. DEADWEIGHT TENSILE TESTS ON POCO-GRAPHITE (AXF-5Q)

of the specimen for producing a pure state of uniaxial tension was discussed. These same problems are inherent in the static tensile fatigue studies and can be remedied only by exercising great care in the preparation of the specimens and the test set up.

## 2. Static Flexural Fatigue

Static flexural fatigue tests are designed to evaluate the effects of sustained loads on the flexural strength of the material. Specimens of ¼ x ¼ x 3 in. long were tested in three-point flexure for a period of 16.67 hr with loads producing a wide variety of stress ranges.

The beam specimens, spanning 2.5 in. between supports were mounted on a frame assembly as shown in Figure 13. A closed hook rider component, placed at midspan carried the platform on which the dead weights to produce the desired stress levels in the beam were placed.

The loads were removed after the given time period had elapsed, and the specimens were carefully examined for any form of permanent surface damage or general deformation suffered under the sustained load. Afterwards they were tested in an Instron testing machine to determine what, if any, stress loss resulted from the sustained load.

## 3. Cyclic Fatigue

If $\sigma_{max}$ and $\sigma_{min}$ are the values of the repeated applied stresses, then the range of stress, R, is defined by:

$$R = \sigma_{max} - \sigma_{min} \tag{20}$$

The cycle of stress is completely defined when the stress range and the maximum stress are known. The average stress, $\sigma_m$, is:

$$\sigma_m = \tfrac{1}{2}(\sigma_{max} + \sigma_{min}) \tag{21}$$

and in the case of complete stress reversal, $\sigma_{max} = -\sigma_{min}$, $R = 2\sigma_{max}$ and $\sigma_m = 0$. By manipulating Eqs. 20 and 21, it can be shown that:

$$\sigma_{max} = \sigma_m + R/2$$
$$\sigma_{min} = \sigma_m - R/2 \tag{22}$$

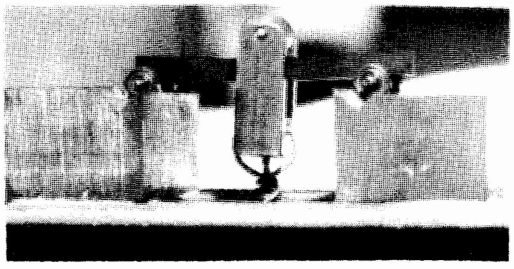

(b) Close Up of Specimen
Under Sustained Load

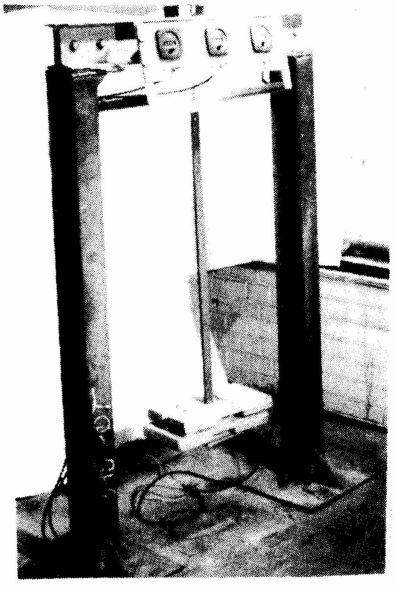

(a) Testing Frame for Sustained
Flexural Loads

Figure 13. DEADWEIGHT FLEXURAL TESTS ON POCO-GRAPHITE (AXF-5Q)

In any endurance test, there are a number of ways in which the loads can be applied to produce varying stress conditions. Of these, two were selected for investigating the cyclic stress of Poco-Graphite.

a. Bending Fatigue

The reversed bending test is probably the most widely accepted method for evaluating fatigue strength of materials. The test consists of applying a known load to the end of a simple cantilever beam and then rotating the beam at constant speed.

The specimens used in this phase of the program were 6 in. long and had a variable cross section as shown in Figure 11. The maximum stress occurs in the smallest diameter starting at the toe of the fillet and extending for a distance of 0.75 in. Effects resulting from stress concentrations are eliminated by using a large radius in the transition from small to large diameters of the specimen.

Since the stress is completely reversed,

$$\sigma_m = 0 \tag{23}$$

and

$$R = 2\sigma_{max} \tag{24}$$

The testing apparatus consists of an electric motor designed to run at a speed of 1800 cpm, a precision loading rig and a counter. A picture of the testing equipment is shown in Figure 14. The specimen to be tested is firmly gripped in the jaws of a chuck attached to the shaft of the electric motor. The loading rig attached to the free end of the cantilever and selected loads to produce desired stress levels are added via the loading rig to the cantilever. A worm and pinion arrangement is used to couple the automatic counter to the motor so that the number of cycles producing failure can be recorded. At the instant of failure, the weight holder on the loading rig falls onto a control switch which immediately cuts off the flow of current to the counter and simultaneously switches off the electric motor.

For each specimen, the distance between the chuck support for the cantilever beam and the point of the load is carefully measured. When the specimen fails, the distance from the face of the chuck to the center of the break is measured. Subtracting this dimension from the load span gives the needed distance from the load to the break point in the specimen. With this data, the maximum flexural stress can be calculated from the well-known formula:

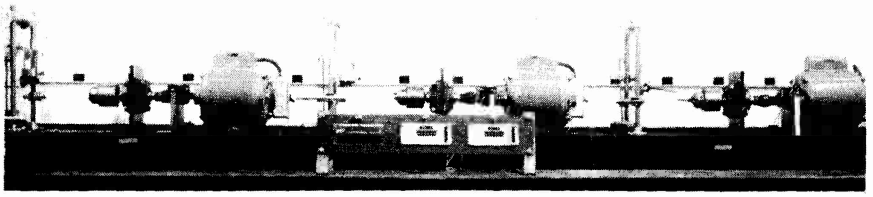

(a) Test Set Up

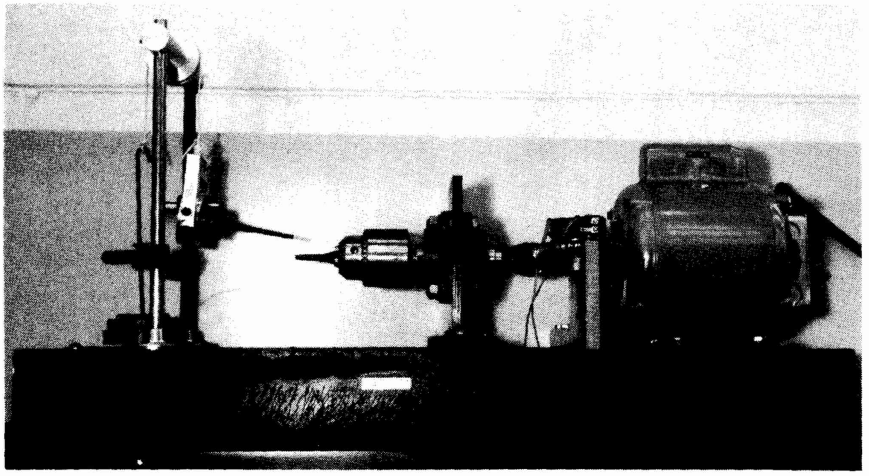

(b) Test Equipment with Failed Specimen

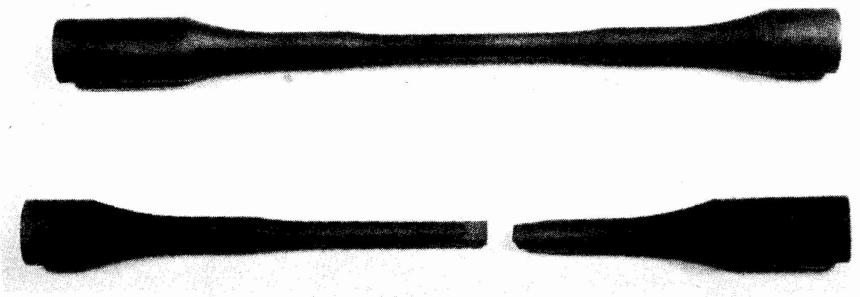

(c) Specimen Before and After Failure

Figure 14. ROTATING BEAM FATIGUE TESTS ON POCO-GRAPHITE (AXF-5Q)

$$\sigma_{flex} = M/S \qquad (25)$$

where M = bending moment at the break point due to the applied load
S = section modulus at the fracture location

This technique for evaluating bending fatigue has the principal advantage of permitting complete control of the test. In addition, the automatic control unit for switching off at failure and keeping a record of the number of cycles is such that it is not necessary to stay with the specimen at all times. Frequent monitoring is all that is necessary so that long periods of time between removal of a failed specimen and installing a new one are not wasted.

b. Torsional Fatigue

Torsional fatigue studies investigated in this program again made use of the principle of complete stress reversal to evaluate the fatigue strength of brittle materials. The test consists of applying a twisting moment first in one direction, then in the opposite direction at one end of a beam which is fixed in position against horizontal movement and rotation about its longitudinal axis.

The specimens used in this phase of the fatigue strength of Poco-Graphite were 4 in. long and had a cross section as shown in Figure 11. As in the case of the specimens used in the rotating beam technique for bending fatigue strength, stress concentration effects were eliminated by thickening the ends of the beams and using large radii in the transition zones. The diameter of the specimen in the gaged length was 0.25 in. with a tolerance of ±0.003 in.

Testing equipment consists of an electric motor operating at 1800 cpm, a sliding bar and cam, a fly wheel, automatic counter and a fixed support. The assembly of the apparatus is shown in Figure 15. The specimen to be tested is firmly gripped at one end in the fixed support as shown in Figure 15. The other end of the specimen is held in a chuck attached to the fly wheel. Movement of the fly wheel is controlled by the sliding bar and cam arrangement mounted on the shaft of the electric motor. By varying the position of the sliding bar on the cam, the angle through which the specimen is twisted can be accurately measured.

To obtain any desired stress level, it is only necessary to measure the angle of twist required to produce fracture of the specimen and relate this to the flexural strength evaluated for the material in the previous work.[13] Since it has been established and demonstrated in many text books on the subject of strength of materials that the angle of twist varies directly as

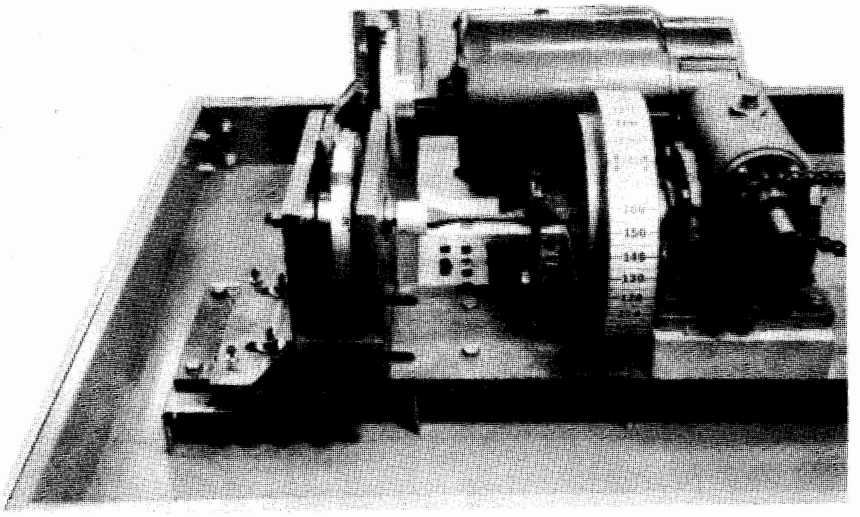

(a) Test Equipment

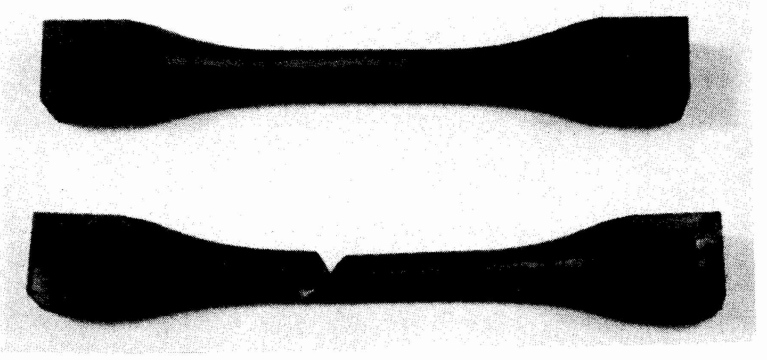

(b) Specimens Before and After Test

Figure 15. TORSIONAL FATIGUE OF POCO-GRAPHITE (AXF-5O)

the applied torque, and hence the applied stress, then by establishing the angle of twist for any specimen, the stress can be calculated from:

$$\sigma_t = \sigma_{ult} \frac{\theta_t}{\theta_{max}} \tag{26}$$

where $\sigma_t$ = stress level for the applied torque
$\sigma_{ult}$ = ultimate strength of the material
$\theta_t$ = applied angle of twist
$\theta_{max}$ = angle of twist required to produce $\sigma_{ult}$

This technique enjoys the same advantages as the rotating beam technique previously described. The only disadvantage is that the apparatus, in its present form must be partially dismantled to mount each new specimen in place. This gives rise to the problem of alignment during reassembly of the equipment. Any misalignment of the specimen can introduce undesirable stresses in the specimen before testing begins.

## C. Energy for Fracture Propagation

The fracture energy of a solid is defined as the energy consumed by the formation of a new surface created during the fracture process. There are several methods for measuring the fracture energy of brittle materials; the two best known being the cleavage technique and the notched beam flexure technique.

### 1. Cleavage Technique

This technique makes use of a double cantilever specimen. The approach to the problem is based on the assumption that the specimen is symmetrical about a horizontal median plane making it equivalent to a pair of opposed identical cantilevers. To eliminate the need for mechanical apparatus to provide external constraint so that the crack, once started, would propagate along the median plane, the thickness of the specimen in this region is reduced by machining fine slots along each face.

The specimens used in the tests conducted in this phase of the program are shown in Figure 16. The double cantilever beams were 6 in. long, 1.5 in. deep at the free end, and 3 in. deep at the loading end. To eliminate the effects of stress concentrations, the transition to the deepened, loading end was made through large radii. Two types of notches were used along the median plane. In the first group of specimens, 60° V-notches 1/16 in. deep were cut in each side of the median plane. The second group of specimens had a 1/16 in. square groove cut on the two sides of the horizontal median plane.

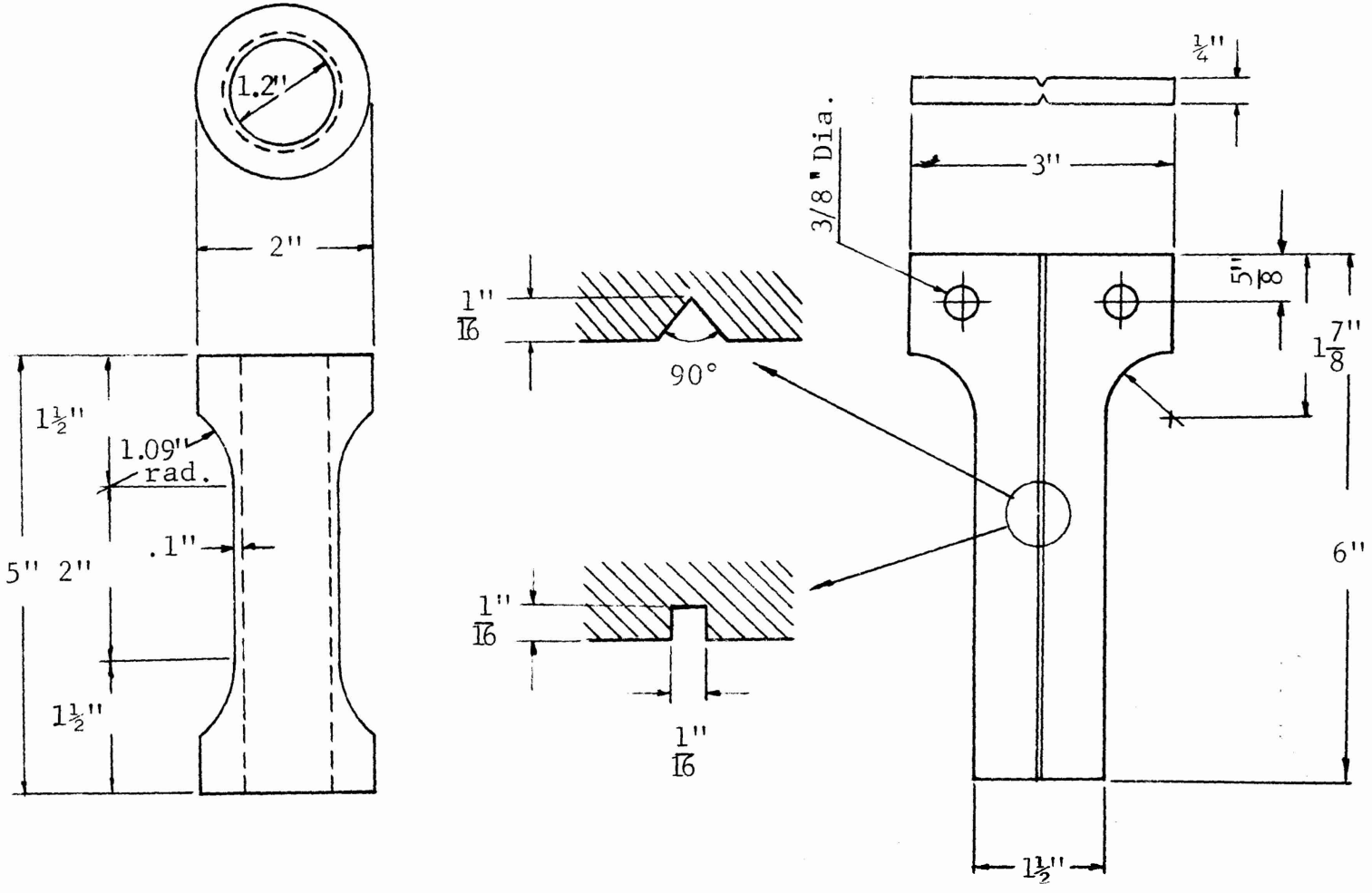


(a) Biaxial Test Specimen

(b) Double-Cantilever Specimens

Figure 16. DETAILS; DOUBLE CANTILEVER AND BIAXIAL SPECIMENS

Ideally, the specimens for this technique should be of constant cross section rather than having a deepened section at the load points. The constant cross section type of specimen, however, presents a problem in load application. To maintain a uniform cross section, the load would have to be applied through some form of friction-type vise grips. For large loads, this type of loading rig was not considered suitable.

If it is assumed that the specimens are to be of uniform depth and that friction type grips cannot be used, then the only other means of applying the load would be through pin and clevis sets. In this loading rig, the pins pass through holes drilled in the specimens, thereby reducing the cross sectional area in this plane. In most cases, the effect of reducing the cross section leads to fracture across the reduced plane before cracking in the median plane develops. For these reasons therefore, the deepened section across the loading plane was considered essential to insure cleavage along the median plane.

The test procedure involved applying increments of load to the specimen mounted in an Instron testing machine as shown in Figure 17. Because cracking occurs very rapidly and without warning, the loads were applied manually so that the instant that cleavage between the two halves of the double cantilever was initiated, loading could be stopped. The length of the initial crack was recorded and small increments of load were applied. After each increment of load crack growth was measured so that the energy required to produce crack propagation could be calculated.

The energy required to initiate cracking by the cleavage technique was investigated by Berry[14] and others.[15] These investigators showed that once the initial crack was formed, the strain energy of the system can be calculated using simple beam theory. By applying the Griffith[1] criteria to the strain energy equation, the energy required to initiate cracking can be calculated from:

$$G = \frac{P\delta n}{4wc} \tag{27}$$

where P = load required to initiate cracking
$\delta$ = the deflection due to P
w = reduced thickness of the median plane
c = crack length
n = a constant derived from the force deflection versus crack length (Figure 18)

The same equation can be used to calculate the energy required to propagate crack growth by substituting,

P = load increment to produce c,
where c = crack growth

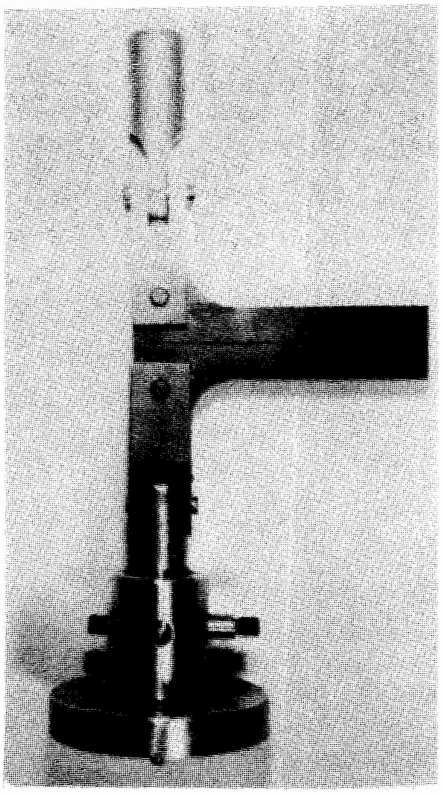


Figure 17. DOUBLE CANTILEVER SPECIMEN ASSEMBLED FOR TESTING

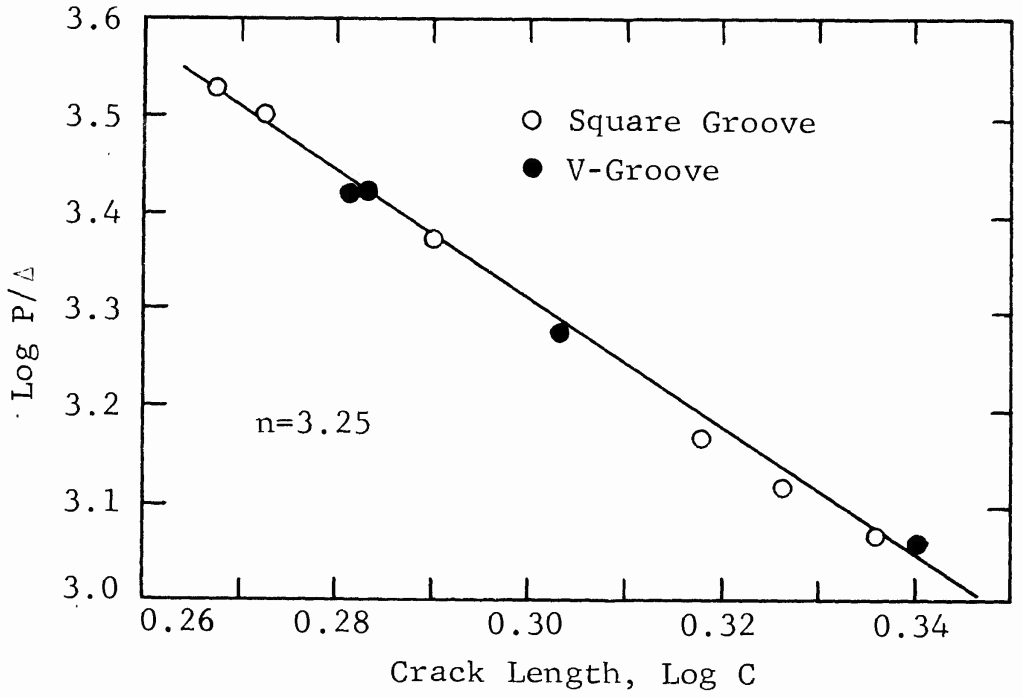


(a) Load/Deflection vs Crack Length for Double Cantilever Beam

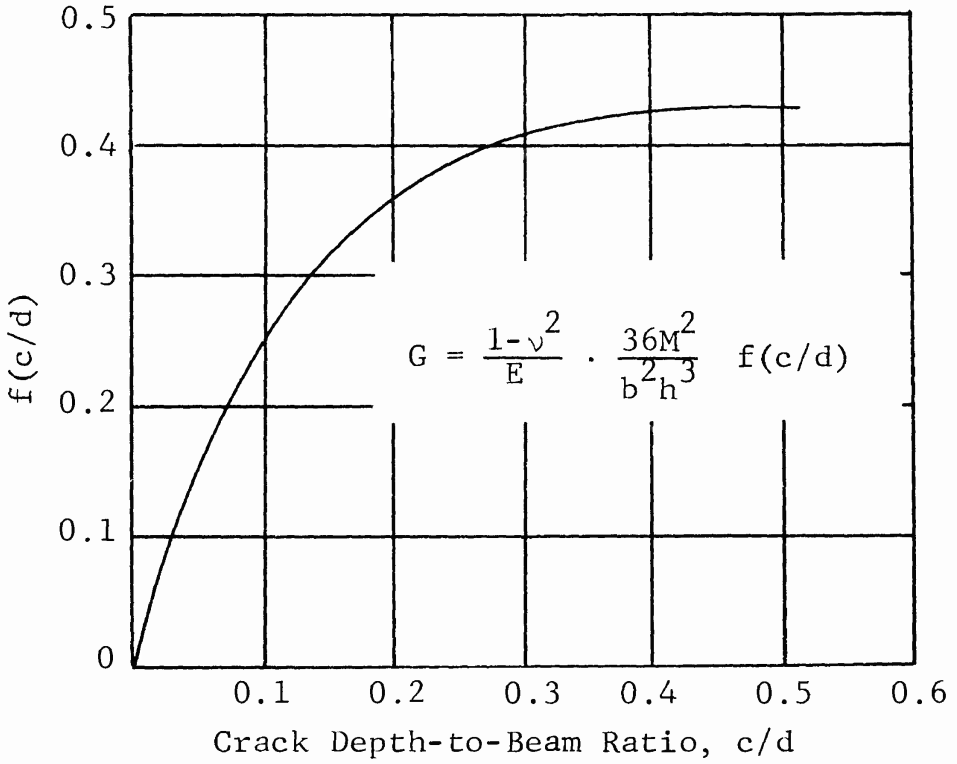


(b) Values of f(c/d) for Different c/d Ratios for Pre-notched Beams

Figure 18. PARAMETERS USED IN EVALUATING ENERGY OF CRACK PROPAGATION

## 2. Bending Technique

As with nearly all of the classic techniques for evaluating fracture toughness or energy of crack propagation of brittle materials, the bending or flexural technique for measuring free surface crack propagation centers around the use of a pre-cracked or pre-notched specimen. Wherever low stress, brittle fracture may possibly occur, the presence of any flaw or defect may give rise to sharp, crack-like characteristics that will influence the design of structural components of brittle materials.

Notched beam specimens of $\frac{1}{4}$ in. square cross section were tested in four-point flexure over a 3 in. span length to evaluate the fracture toughness of Poco-Graphite. Four-point loading is used in this technique for two reasons. First, the shear due to the applied loads is zero at midspan (where the notch is located) and is not a factor to be accounted for in analysis of the results. Second, loading in this manner takes a load point away from the notched section of the beam thus reducing the probability of a premature failure due to a high shear and bending stresses at the tip of the notch; an area of high stress concentrations.

The use of the notched specimen in this technique is based on the Griffith concept that rapid crack propagation will commence from a stationary crack when the strain energy release rate becomes equal to some critical value referred to as the fracture toughness of the material.

The strain energy release rate was defined earlier as the change in elastic strain energy when a new crack surface is formed. On this basis, therefore, it should be possible to calculate the stress distribution in the notched specimen by the theory of elasticity. The strain energy release rate would then be defined as the partial derivative of the total strain energy with respect to the depth of the crack.[16] Griffith used the elastic analysis approach to show that strain energy release rate is given by:

$$G = \frac{\pi \sigma^2 c}{E} \tag{28}$$

where $\sigma$ = stress due to the applied load
$c$ = depth of crack
$E$ = modulus of elasticity

Winne and Wundt[17] used the Griffith criteria to develop an expression for calculating the fracture energy of a pre-notched beam in flexure:

$$G = \frac{(1 - \nu^2)}{E} \cdot \sigma_n^2 h \cdot f(c/d) \tag{29}$$

where $\sigma_n$ = nominal bending stress at the root of a crack
$\nu$ = Poisson's ratio as determined from flexural test data
h = depth of the member above the crack
f(c/d) = function of c/d as shown in Figure 18

If $\sigma_n$ is written in terms of the bending moment, M, at the center of the beam, then the fracture energy can be calculated from:

$$G = \frac{1 - \nu^2}{E} \cdot \frac{36M^2}{b^2h^3} \, f(c/d) \qquad (30)$$

A compliance analysis method described by Corum[16] yielded results for four-point flexure tests on EGCR-Type Agot Graphite that were essentially the same as those obtained using the elastic analysis based on the Griffith criteria. Since compliance testing supported the elastic analysis, it was decided to use the latter method for calculating the strain energy release for crack initiation for the tests made on the Poco-Graphite beams in flexure.

D. Biaxial Tests

It is difficult to visualize a structure in which any member is subjected to the action of a uniaxial stress alone. Hence, it is vitally important to make experimental data available for brittle materials under the action of polyaxial states of stress. The purpose of this phase of the present program was to develop a biaxial tension-compression technique for brittle materials in which the stress distribution could be accurately known and the failure would occur in the test section of the specimen.

The specimen selected for the tests was a hollow cylinder having an internal diameter of 1.2 in. and an external diameter of 1.4 in. in the test section. The ends of the cylinder were thickened to a diameter of 2.00 in. so that the ratio of wall thickness in the end zones to that of the gaged length was 4:1. Effects of stress concentrations were eliminated by using a large radius in the transition from thin-to-thick wall thickness. Total length of the specimens was 5 in. and a sketch and picture of a specimen is shown in Figure 16.

This type of specimen with many variations has been used extensively in biaxial tension-compression tests. Generally, the major problems with this technique are associated with the end zones where end plugs are used to seal the specimen and with the degree of restraint arising from high axial loads.

The problem of the end plugs is usually one of economics rather than lack of design ability. The specimens for any biaxial

test program are difficult to prepare and costly to machine. The making of end plugs to provide a perfectly smooth interior contour in the specimen would then be extremely expensive and would limit the number of specimens available for testing considerably. As a result of this, the end plugs designed for these tests have provided small areas of high stress concentrations in the specimen.

Internal pressure is applied via a hydraulic system through a rubber balloon, shown in the exploded view of the test set up (Figure 19), and as the pressure increases, the balloon tends to be molded into the shape of the interior contour of the specimen. Hence, if the end plug does not provide a perfectly smooth contour, stress concentrations will be introduced into the specimen at the junction of the interior wall of the cylinder and the end plug.

For a valid test in a biaxial state of stress, it is important that the vertical load is distributed over the entire cross section of the specimen. To achieve this is not easy since it demands extreme accuracy in machining the specimen so that the horizontal planes are true and normal at all levels to the vertical axis. In addition the loading head and carrier plate on the testing machine must also be of high precision accuracy. These limits of accuracy are generally not attainable for average test conditions, and hence, errors of varying magnitude are present in the test data when high compressive loads are used.

In view of these two unfavorable factors it was decided that, for the limited number of specimens available for testing,

1. A rubber membrane would be used for sealing the end of the specimen rather than a fitted end cap, and

2. Lower axial loads would be applied as a measure of acceptability of the technique for future work.

The testing technique involved the application of vertical and internal pressure on the specimen, to introduce a state of biaxial tensile-compressive stress. A rubber balloon, seen in Figure 19 was the medium through which the interval pressure was applied.

The testing apparatus, shown in Figure 20, consisted of a Tinius-Olsen universal testing machine set up to provide compressive forces in the vertical plane of the specimen, a hand operated hydraulic pump to introduce the internal pressure into the balloon and recording equipment to monitor tensile and compressive strains in certain specimens gaged with Budd electric resistance SR-4 strain gages.

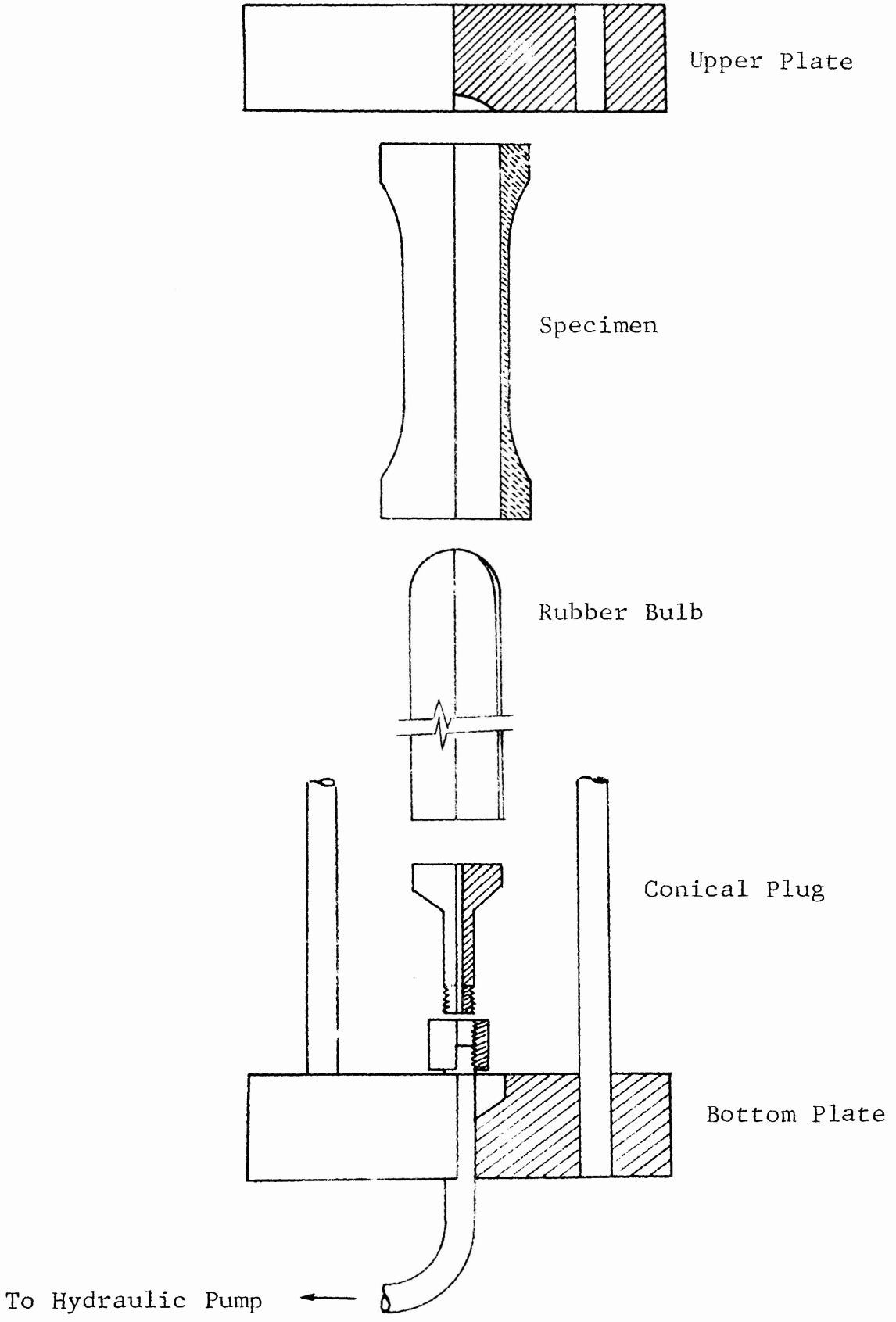


Figure 19. EXPLODED VIEW OF BIAXIAL TEST

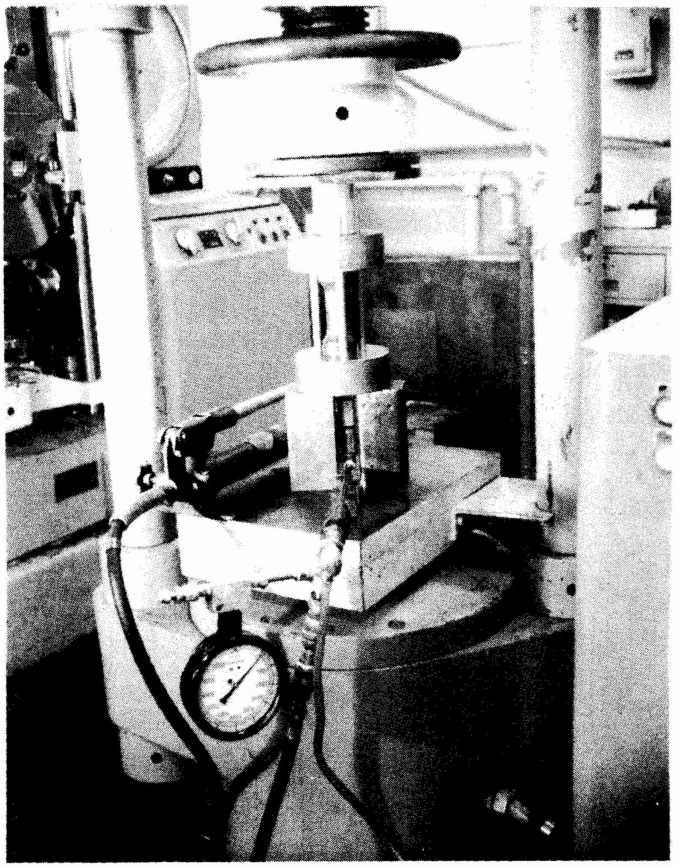

(a) Test Equipment

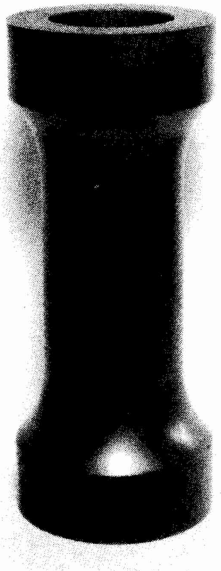

(b) Before Test

(c) Typical Failure

Figure 20. BIAXIAL TESTS OF POCO-GRAPHITE (AXF-5Q)

Prior to testing the interior of the specimen the ends of the cylinder were carefully cleaned to remove any foreign particles from the surfaces to be subjected to stress. The ends were then sealed with rubber membranes stretched over the specimens. The bottom membrane had a small hole in it through which the rubber balloon was passed. The nipple on the end of the hydraulic line from the hand pump and over which the balloon was tightly secured to prevent any leaks, was forced through the small hole in the lower membrane. A small amount of pressure was applied by the hand pump to check for leaks in the system.

The specimen was carefully positioned on the upper and lower platens of the testing machine (Figure 20) to ensure as accurate alignment as possible.

To investigate the effects of applying the internal pressure simultaneously with the compressive load four specimens were tested by first applying a small axial load (50 lb) and then introducing the internal pressure with the hand pump. The vertical load resulting from this procedure was monitored on the scaled dial of the Tinius-Olsen testing machine.

The remainder of the specimens were tested by first applying a predetermined axial force by the Tinius-Olsen machine. When this load was reached it was maintained constant during the application of the internal pressure until failure occurred. The reason for this was to prevent a build up of excessive axial stress due to the internal pressure and hence high degrees of end restraint between the specimen and the testing machine.

## IV. TEST RESULTS

The results of the tests conducted in this program are presented in both tabular and graphic form for each type of test represented. The tabular data for all tests are presented in Appendix A.

### A. Impact Test Results

Figures 8, 9 and 21 show the apparatus used and typical fractures for each impact test evaluated. Table I summarizes the test data for this part of the program.

#### 1. Swinging Pendulum Tests

The first impact tests were made on notched and un-notched specimens using the 50 in.-lb Izod pendulum. Calibration of this pendulum showed that machine losses amounted to only 0.12 in.-lb as discussed in the previous section. Results obtained from testing 30 un-notched specimens exhibited an average impact energy of 1.6 in.-lb with a standard deviation of 0.22 in.-lb and a coefficient of variation of 13.5%.

Following these tests on un-notched specimens, 15 notched specimens were tested using the same pendulum. For the notched specimens the average impact energy was 0.55 in.-lb with a deviation of 0.1 in.-lb representing a variation of 1.75%.

These initial tests indicated that despite the low resolution of the testing machine, it is still a significant factor in evaluating the impact strength of Poco-Graphite.

The second series of impact tests was next made with the 17.19 in.-lb Izod pendulum. For this head, the machine losses amount to 2.58 in-lb, considerably higher than those exhibited by the heavier pendulum. Fifty un-notched specimens tested with this lighter pendulum yielded an average impact energy for Poco-Graphite of 1.8 in.-lb, a 12½% increase over the 1.6 in.-lb averaged with the 50 in.-lb pendulum. The coefficient of variation in impact energy also increased when the lighter head was used to a value of 20.2%. This figure represents a 50% increase in variation over the results obtained with the heavier pendulum.

Although the results of the Izod tests on un-notched specimens using both the heavy and light pendulums are in reasonably good agreement, the wide scatter in the data obtained from these tests seem to indicate that the resolution of the testing equipment is a significant factor in evaluating the impact energy of brittle materials. The presence of bearings, rider indicators and a release mechanism all create variations in pendulum energy

(a) Notched Charpy Specimen

(b) Un-notched Izod Specimen

(c) Un-notched Drop Weight Specimen

Figure 21. FRACTURED SPECIMENS AFTER IMPACT TESTS ON POCO-GRAPHITE (AXF-5Q)

Table I

SUMMARY OF IMPACT TESTS ON POCO-GRAPHITE (AXF-5Q)

| Test | Number tested | Average energy (in.-lb) | Standard deviation (in.-lb) | Coefficient of variance (%) | Average machine loss (in.-lb) |
|---|---|---|---|---|---|
| 50 in.-lb Izod, Free Swing | 50 | 49.88 | 0.18 | 0.36 | 0.12 |
| 50 in.-lb Unnotched Izod | 30 | 1.60 | 0.22 | 13.52 | -- |
| 50 in.-lb Notched Izod | 15 | 0.55 | 0.096 | 17.50 | -- |
| 17.19 in.-lb Izod, Free Swing | 50 | 14.61 | 0.47 | 3.24 | 2.58 |
| 17.19 in.-lb Unnotched Izod | 50 | 1.80 | 0.36 | 20.20 | -- |
| 18.32 in.-lb Charpy, Free Swing | 50 | 17.23 | 0.22 | 1.29 | 1.10 |
| 18.32 in.-lb Unnotched Charpy | 50 | 1.71 | 0.37 | 21.77 | -- |
| 18.32 in.-lb Notched Charpy | 50 | 0.32 | 0.29 | 91.24 | -- |
| Drop Weight | 296 | 1.388 | 0.062 | 4.50 | 0 |

which, being an integral part of the kinetic energy give unreliable values for the impact strength of the material.

The third series of impact tests were made using the same Tinius-Olsen testing machine but equipped with a Charpy 18.32 in.-lb pendulum. Machine losses for this pendulum were considerably less than those exhibited by the Izod 17.19 in.-lb pendulum but still of a much higher order of magnitude than those of the 50 in.-lb Izod tester.

Fifty un-notched specimens in the Charpy test yielded an average impact strength for Poco-Graphite of 1.71 in.-lb with a standard deviation of 0.37 in.-lb and a variation of 21.77%. These results were in excellent agreement with the Izod test using the 17.19 in.-lb pendulum. When compared with the results from the Izod tests using the heavy hammer, correlation was also very good, except that the variation in the data was still 50% greater for the Charpy light pendulum tests than for the Izod tests.

Thirty notched specimens were tested with the Charpy impact testing equipment. The results averaged 0.32 in.-lb impact energy but with a variation in the data of 91.25%. The impact strength for un-notched specimens in these Charpy tests was therefore 40% less than that for similar tests with the Izod 50 in.-lb pendulum. This rather large difference can be attributed in part to the position of the notch with respect to the point in the beam where the pendulum head strikes. In the Izod test, the notch is a small distance away from the pendulum head, whereas the Charpy head strikes the specimen immediately behind the notch. The Charpy specimens therefore exhibit the effect of stress concentrations arising from stress raisers at the load point.

The wide scatter obtained in the Charpy test data is again indicative of the influence of the resolution of testing apparatus in evaluating the impact strength of brittle materials.

The notch sensitivity ratio (NSR) of the Poco-Graphite calculated from Eq. 19 was determined for the Izod test to be;

$$NSR = \frac{K_u}{K_n} = \frac{1.6}{0.55} = 3.00$$

and for the Charpy test,

$$NSR = \frac{K_u}{K_n} = \frac{1.71}{0.32} = 5.34$$

The higher value obtained for the Charpy tests illustrates the combined notch effects caused by the impact load at the point of contact on the specimen plus the stress concentrations resulting from the preformed V-notch. The notch sensitivity ratio was 75% greater than for the Izod test.

## 2. Drop Weight Tests

The drop weight tests for determining the impact strength of brittle materials involved a larger number of specimens than either the Charpy or Izod tests. The reason for this is due to the different form of analyzing the test data. Whereas the pendulum-type tests involved a fixed position of the impact load, the drop weight tests are based on the probability of failure due to variations in the height from which the impact force is permitted to fall. With this test one can determine the energy range for zero failures and for 100% failures for a given sampling of the entire population.

A total of 296 specimens were tested and the results are tabulated in Table A-I. No failures occurred when the 0.619 lb steel ball was dropped from a height of 19.99 in. on a sample population of 10 specimens. From this point on, raising the position of the weight increased the probability of failure for any sampling of the population until a level was reached where 100% failure occurred.

Close inspection of the accumulated data revealed that small variations in density appeared to influence the percentage of failures occurring at any level of energy. It was therefore considered necessary to evaluate the probability of failure for a range of energy levels rather than at any one discreet level. This is illustrated in the third column of Table A-II and again in Figure 22 where the probability of failure is plotted as a function of the energy/density ratio.

The mean weighted average impact energy calculated from the average density of all specimens tested was 1.388 in.-lb with a standard deviation of only 0.062 in.-lb and a coefficient of variation of only 4.5%.

Drop weight testing yielded a lower average impact strength than either the Charpy or Izod tests. The 1.388 in.-lb average value of impact energy by drop weight testing was 20% lower than the Izod light pendulum energy value of 1.8 in.-lb, 12.5% less than the heavy pendulum Izod value of 1.6 in.-lb and 18% less than the Charpy test impact energy value of 1.71 in.-lb. These differences are accounted for in part by the mechanical losses in the test equipment. However, they do not take into account flaws and surface defects in the specimens nor do they account for micro-cracks which may occur on impact. The drop weight technique, on the other hand, by evaluating probability of failure as a criteria for evaluating impact strength does to a certain degree account for these effects. In view of the fact that the percent variation in the drop weight test data is only about one quarter of the variation exhibited in the swinging pendulum tests, it is felt that this technique gives a more reliable indication of the impact strength of Poco-Graphite.

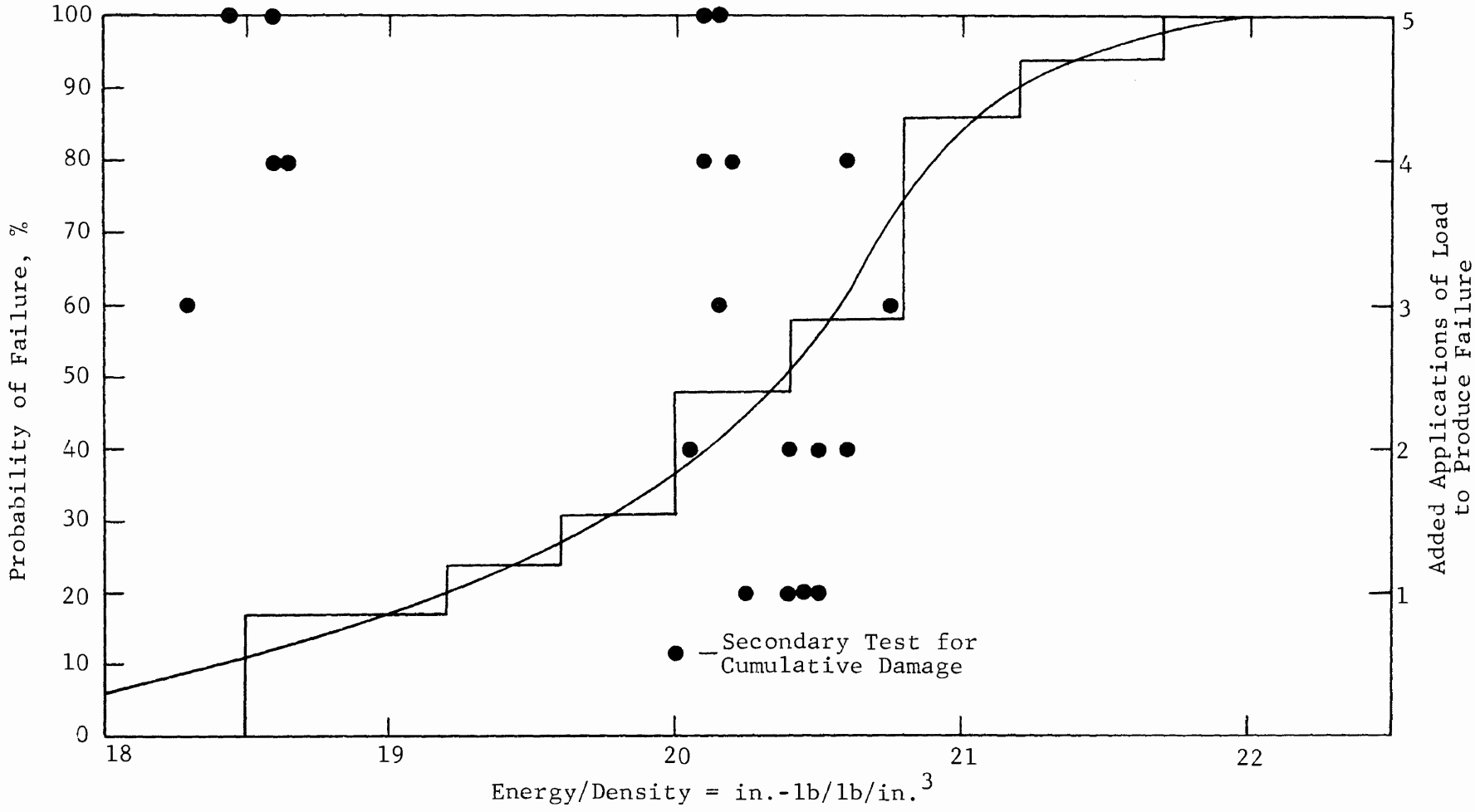


Figure 22. IMPACT STRENGTH OF POCO-GRAPHITE (AXF-5Q) BY DROP WEIGHT TESTING

### 3. Effects of Cumulative Damage

The next step in the impact testing of the material was to evaluate the effects of cumulative damage to repeated applications of the impact load.

For the drop weight tests, 20 specimens which did not fail in the initial impact test were subject to repeat applications of the dynamic load originally applied. The results of these tests are shown in Table II and also in Figure 22. The specimens were randomly selected and included beams which had been subjected to low impact energy as well as to the higher values of impact energy. All of the specimens failed at between one and five additional load applications giving rise to the postulation that cumulative damage does affect the impact strength of Poco-Graphite. However, no fixed pattern of repeated applications to failure versus impact energy was exhibited. Regardless of the value of the impact energy the range of repeated applications of load to produce failure remained about the same.

Swinging pendulum tests were also made to evaluate the effects of cumulative damage. Ten notched and un-notched specimens were tested using both the Charpy and the Izod heads. The results of these tests, shown in Table II show that repeated applications of a dynamically applied load reduce the impact strength of Poco-Graphite. With the Izod pendulum, repeated applications of load showed a reduction of 18% for both the notched and un-notched specimens. The new average values were 0.463 and 1.490 in.-lb compared to 0.550 and 1.800 in.-lb recorded for a single swing of the pendulum.

Similar results were observed for the tests made with the Charpy head. After repeated applications of load, the average impact energy was 0.288 and 1.340 in.-lb, respectively for notched and un-notched specimens. These show reductions of 15 and 20% against the values of 0.32 and 1.71 in.-lb for the single swing of the pendulum.

The final test in this phase of the program was to investigate the effects of a dynamically applied load on the flexural strength of the material. Ten specimens previously tested by the drop weight technique were tested in four-point flexure to evaluate this effect. The results of these tests, shown in Table III, gave an average flexural strength of 11,290 psi. In the previous study,[13] the average strength of Poco-Graphite tested in four-point flexure was reported to be 13,385 psi. On this basis, it appears that a dynamic load, applied only one time, reduces the flexural strength by about 10%. This series of tests undergo reductions due to cumulative damage of repeated load applications. While the exact nature of this weakening effect is difficult to evaluate, it is believed to be associated with micro-cracking dislocation movement.

Table II

SUMMARY OF REPEATED IMPACT LOADS ON POCO-GRAPHITE (AXF-5Q)

| Test | Number of specimens | Average energy (in.-lb) | Standard deviation (in.-lb) | Variation (%) | Average number of strikes |
|---|---|---|---|---|---|
| Drop Weight, Unnotched | 20 | 1.348 | 0.047 | 3.49 | 3 |
| Unnotched Izod | 10 | 1.490 | 0.065 | 4.36 | 8 |
| Unnotched Charpy | 10 | 1.348 | 0.056 | 4.16 | 10 |
| Notched Izod | 10 | 0.451 | 0.038 | 8.43 | 11 |
| Notched Charpy | 10 | 0.287 | 0.013 | 3.55 | 8 |

Table III

FOUR-POINT FLEXURAL TESTS AFTER IMPACT
LOAD ON POCO-GRAPHITE (AXF-5Q)

| Specimen number | Load (lb) | Stress (psi) | Standard deviation (psi) | Coefficient of variance (%) |
|---|---|---|---|---|
| 1 | 92 | 13,270 | --- | --- |
| 4 | 80 | 11,540 | --- | --- |
| 38 | 72 | 10,380 | --- | --- |
| 75 | 88 | 12,670 | --- | --- |
| 79 | 70 | 10,115 | --- | --- |
| 136 | 85 | 12,260 | --- | --- |
| 201 | 70 | 10,115 | --- | --- |
| 249 | 70 | 10,115 | --- | --- |
| 282 | 80 | 11,540 | --- | --- |
| 283 | 75.5 | 10,880 | --- | --- |
| Average Stress | | 11,290 | 960 | 8.5 |

## B. Fatigue Test Results

### 1. Static Fatigue

The pin loaded tensile specimens tested under sustained loads for time periods ranging from 100 to 400 hr showed no indication of static fatigue. Eighteen specimens tested in air at room temperature under loads producing tensile stresses ranging from 25 to 98% of the ultimate strength as evaluated by tests made on the billet showed no drop in ultimate tensile strength when tested in the Instron testing machine. Five additional specimens stored in an atmosphere of pure oxygen for 100 hr exhibited similar characteristics.

The results of these tests, shown in Table IV indicate that neither static tensile fatigue nor cumulative damage due to sustained load exists in Poco-Graphite. These results are important to the cyclic fatigue phase since they eliminate the variables of atmospheric attack and time-under-load effects.

Seventeen specimens were tested for static fatigue in three-point flexure with midspan loads selected to give a range of flexural stress from 17 to 90% of the ultimate strength of the material.

The specimens were kept under observation for 16.67 hr before being unloaded. Visual observation of the specimens disclosed no apparent surface defects resulting from the sustained flexural loads. No permanent measurable deformations were present in the specimens. After careful visual examination was completed, each specimen was tested in three-point flexure on roller supports to determine if the sustained loads had any affects on the flexural strength of the material.

When compared with the data from similar tests given in the previous report(13) the flexural strength of these specimens showed a reduction of about 15% as noted in Table V.

Two specimens were kept under observation for 250 hr under loads of 67 and 80% of the ultimate strength of the material. Again no visible signs of distress were observed, and the reduction in strength when tested to failure was of the same order of magnitude as the other specimens.

When a beam is tested in flexure, the portion above the neutral axis is in compression while the portion below the neutral axis is in tension. It has already been shown that the ultimate tensile strength of Poco-Graphite is unaffected by sustained loads and Ely(18) has shown that the ultimate compressive strength of

Table IV

DEAD WEIGHT TENSILE FATIGUE TESTS
ON POCO-GRAPHITE (AXF-5Q)

| Specimen number | Stress (psi) | Time under stress (hr) | Result | Tensile strength test (psi) |
|---|---|---|---|---|
| 2 | 2319 | 120 | No break | 9709 |
| 8 | 4472 | 120 | No break | 9734 |
| 14 | 6723 | 400 | No break | 9622 |
| 8* | 7090 | 280 | No break | 9734 |
| 2* | 7570 | 280 | No break | 9709 |
| 20 | 7965 | Failed when No. 3 fell (19 min) | | -- |
| 15 | 8205 | 100 | No break | 9552 |
| 4 | 8252 | 118 | No break | 9069 |
| 21 | 8445 | Failed at pin | | -- |
| 6 | 8508 | 400 | No break | 9930 |
| 12 | 8752 | 400 | No break | 9948 |
| 16 | 8801 | 319 | No break | 9256 |
| 18 | 8825 | 168 | No break | 9480 |
| 10 | 8826 | 320 | No break | 10,080 |
| 18* | 8841 | 100 | No break | 9480 |
| 22 | 8849 | Instantaneous | | -- |
| 9 | 8852 | Instantaneous | | -- |
| 3 | 8865 | Instantaneous | | -- |
| A-19** | 7116 | 100 | No break | 9140 |
| A- 7** | 7719 | 100 | No break | 9249 |
| A- 1** | 8329 | 100 | No break | 7936*** |
| A- 9** | 8487 | 140 | No break | 8063*** |
| A- 2** | 8680 | Instantaneous | | -- |
| A-15** | 8959 | Instantaneous | | -- |
| A-21** | 8959 | 118 | No break | 9079 |
| A-20** | 8999 | Instantaneous | | -- |
| A- 8** | 9188 | Instantaneous | | -- |
| A-13 | Tested on Instron to determine strength of billet. | | | 9040 |
| A-14 | | | | 9650 |
| A-17 | | | | 9601 |

*Increased loads on original specimen.

**Tested in pure oxygen, all others tested at room environment in air.

***Apparently damaged on removal from static test fixture.

Table V

DEAD WEIGHT FLEXURAL FATIGUE TESTS
IN AIR ON POCO-GRAPHITE (AXF-5Q)

| Specimen number | Stress (psi) | Time under stress (min) | Result | Flexural strength test (psi) |
|---|---|---|---|---|
| 1 | 2030 | 1140 | No break | 12,000 |
| 2 | 2640 | 1146 | No break | 13,200 |
| 3 | 2640 | 1000 | No break | 10,800 |
| 4 | 3840 | 1000 | No break | 10,800 |
| 5 | 6480 | 1180 | No break | 12,000 |
| 6 | 6480 | 1180 | No break | 13,400 |
| 7 | 7200 | 1000 | No break | 14,400 |
| 8 | 7200 | 1000 | No break | 13,200 |
| 9 | 7680 | 1330 | No break | 10,500 |
| 10 | 7680 | 1330 | No break | 13,400 |
| 11 | 8200 | 1007 | No break | 12,900 |
| 12 | 8200 | 1007 | No break | 10,800 |
| 13 | 8880 | 15,470 | No break | 13,200 |
| 14 | 8880 | 15,470 | No break | 11,040 |
| 15 | 9360 | 340 | Broke* | -- |
| 16 | 9360 | 1007 | No break | 13,400 |
| 17 | 10,800 | 1221 | No break | 12,000 |

*Additional weights added after 5 hr causing an instantaneous break.

fine-grained graphite is reduced under slow-loading rates at room temperature. Therefore, it is theorized that this reduction in flexural strength is due to weakened flexural planes in sustained compression.

The results obtained from the static flexural tests indicate a definite need for additional work on the effects of sustained loads in both flexure and compression. For such an investigation, size and shape should be considered along with end restraint and support conditions. Flexural specimens not failing under sustained loads should be tested to failure in the opposite direction (tension plane in compression) for a full evaluation of strength reduction.

2. Cyclic Fatigue

Tables VI and VII summarize the test data obtained from the cyclic fatigue data and Figures 23 and 24 show the graphical interpretation of these data.

The rotating beam tests, designed to evaluate the flexural fatigue properties of Poco-Graphite were run at a frequency of 1500 cpm at room temperature and humidity. The deflection of the loaded end and the location of the center of the break at fracture were used to calculate the failure stress in each specimen. As seen in the S-N curve of Figure 23, the scatter in the test data was rather large and led to the establishing of an upper and lower bound for the S-N curve rather than the usual single line curve associated with elastic materials. In view of the data obtained from the impact tests and the previously reported uniaxial and flexural tests, this scatter in the data which lies enclosed in the envelope of the upper and lower limits was anticipated for the cyclic fatigue tests.

The vertical spread (range of stress for a given number of cycles of load repetition) of the upper and lower boundaries of the S-N curves is approximately constant. This fact tends to indicate that the scatter in the data is related to material variations rather than the testing technique used. The spread was about 3000 psi.

Similar results were observed for the torsional fatigue tests as shown in Figure 24. The scatter in the data obtained from these tests was also such that an upper and lower limit for cyclic fatigue of Poco-Graphite was established on the S-N curve. Fewer specimens were tested in torsional cyclic fatigue than in flexural cyclic fatigue, but the similarity in the trends of the plotted data are directed toward the same conclusions.

The agreement between the behavior of the material in torsional fatigue and in flexural fatigue is illustrated in Figure 25 where the results of the two tests have been incorporated

Table VI

ROTATING BEAM FLEXURAL FATIGUE
OF POCO-GRAPHITE (AXF-5Q)

| Specimen number | Stress (psi) | Number of Cycles |
|---|---|---|
| 1 | 15,781 | Static |
| 2 | 9006 | 2220 |
| 3 | 8658 | 600 |
| 4 | 14,863 | Static |
| 5 | -- | 10,000,000* |
| 6 | -- | 10,056,000* |
| 7 | -- | 10,030,000* |
| 8 | 8516 | 860 |
| 9 | 8437 | 1500 |
| 10 | 7931 | 8420 |
| 11 | 9317 | 2820 |
| 12 | 9377 | 1540 |
| 13 | 17,117 | Static |
| 14 | 6810 | 4840 |
| 15 | 7308 | 106,140 |
| 16 | -- | 15,000,000* |
| 17 | 9271 | 400 |
| 18 | 9150 | 320 |
| 19 | 8697 | 640 |
| 20 | 7142 | 9400 |
| 21 | -- | 15,000,000* |
| 22 | -- | 15,000,000* |
| 23 | 7700 | 2880 |
| 24 | 8562 | 1320 |
| 25 | 8214 | 1960 |
| 26 | 8790 | 5,800,000* |
| 27 | 8525 | 780 |
| 28 | 8909 | 2140 |
| 29 | 9013 | 1400 |
| 30 | 14,504 | Static |
| 31 | 8939 | 1800 |
| 32 | 9250 | 180 |
| 33 | 7918 | 120 |
| 34 | 9368 | 1300 |
| 35 | -- | 10,100,000* |
| 36 | 9960 | 1 |
| 37 | 9450 | 60 |
| 38 | 10,634 | 20 |
| 39 | 11,470 | 120 |
| 40 | 14,963 | Static |

Table VI (Cont'd)

ROTATING BEAM FLEXURAL FATIGUE
OF POCO-GRAPHITE (AXF-5Q)

| Specimen number | Stress (psi) | Number of Cycles |
|---|---|---|
| 41 | 10,614 | 5 |
| 42 | 8199 | 380 |
| 43 | 11,499 | 70 |
| 44 | 11,140 | 1 |
| 45 | 15,199 | Static |
| 46 | 11,470 | 2 |
| 47 | 10,260 | 210 |
| 48 | 9691 | 190 |
| 49 | 10,377 | 35 |
| 50 | 10,040 | 4 |
| 51 | 10,381 | 4 |
| 52 | 10,706 | 170 |
| 53 | 13,870 | Static |
| 54 | 10,480 | 65 |
| 55 | 10,230 | 90 |
| 56 | 10,932 | 30 |
| 57 | 9440 | 590 |
| 58 | 9376 | 48,825 |
| 59 | 14,297 | Static |
| 60 | 13,320 | Static |
| 61 | 10,430 | 45 |
| 62 | 9513 | 40 |
| 63 | 9721 | 60 |
| 64 | 10,631 | 20 |
| 65 | 13,723 | Static |
| 66 | 12,137 | 10 |
| 67 | 11,147 | 10 |
| 68 | 11,256 | 10 |
| 69 | 10,570 | 60 |
| 70 | 9997 | 65 |
| 71 | 10,423 | 55 |
| 72 | 9750 | 130 |
| 73 | 14,940 | Static |
| 74 | 8705 | 420 |
| 75 | 8547 | 625 |
| 76 | -- | 10,000,000* |
| 77 | -- | 10,000,000* |
| 78 | -- | 1,359,000 |
| 79 | 16,815 | Static |

*No break.

Table VII

CYCLIC TORSIONAL FATIGUE
OF POCO-GRAPHITE (AXF-5Q)

| Specimen number | Stress (psi) | Number of Cycles |
|---|---|---|
| 1 | 3960 | 6,831,000 |
| 2 | 11,460 | 25 |
| 3 | 11,460 | 25 |
| 4 | 11,460 | 20 |
| 5 | 11,460 | 180 |
| 6 | 11,460 | 135 |
| 7 | 9290 | 170 |
| 8 | 9290 | 130 |
| 9 | 9290 | 35 |
| 10 | 9290 | 45 |
| 11 | 9290 | 48,080 |
| 12 | 7160 | 880 |
| 13 | 7160 | 370 |
| 14 | 9290 | 170 |
| 15 | 9290 | 1500 |
| 16 | 7160 | 630 |
| 17 | 7160 | 840 |
| 18 | 7160 | 97,610 |
| 19 | 4990 | 231,130 |
| 20 | 4990 | 3,369,800 |
| 21 | 4990 | 750 |
| 22 | 4990 | 150 |
| 23 | 4990 | 2,538,600* |
| 24 | 5730 | 1,210,460 |
| 25 | 6440 | 1635 |
| 26 | 6440 | 865 |
| 27 | 6440 | 200 |
| 28 | 6440 | 5480 |

Table VII (Cont'd)

CYCLIC TORSIONAL FATIGUE
OF POCO-GRAPHITE (AXF-5Q)

| Specimen number | Stress (psi) | Number of Cycles |
|---|---|---|
| 29 | 5730 | 2,555,150* |
| 30 | 7870 | 70 |
| 31 | 7870 | 45 |
| 32 | 7870 | 40 |
| 33 | 7870 | 60 |
| 34 | 7870 | 85 |
| 35 | 8580 | 45 |
| 36 | 8580 | 20 |
| 37 | 8580 | 105 |
| 38 | 8580 | 55 |
| 39 | 8580 | 70 |
| 40 | 15,740 | Static |
| 41 | 14,300 | Static |
| 42 | 17,900 | Static |
| 43 | 5730 | 3,459,500* |
| 44 | 5730 | 7370 |
| 45 | 5730 | 2,882,230 |
| 46 | 5730 | 2,843,535* |
| 47 | 8240 | 225 |
| 48 | 8240 | 180 |
| 49 | 8240 | 25 |
| 50 | 7500 | 45,070 |
| 51 | 7500 | 400 |
| 52 | 7500 | 5500 |
| 53 | 6780 | 5,000,000* |
| 54 | 6780 | 5,000,000* |
| 55 | 6780 | 5,000,000* |

*No break.

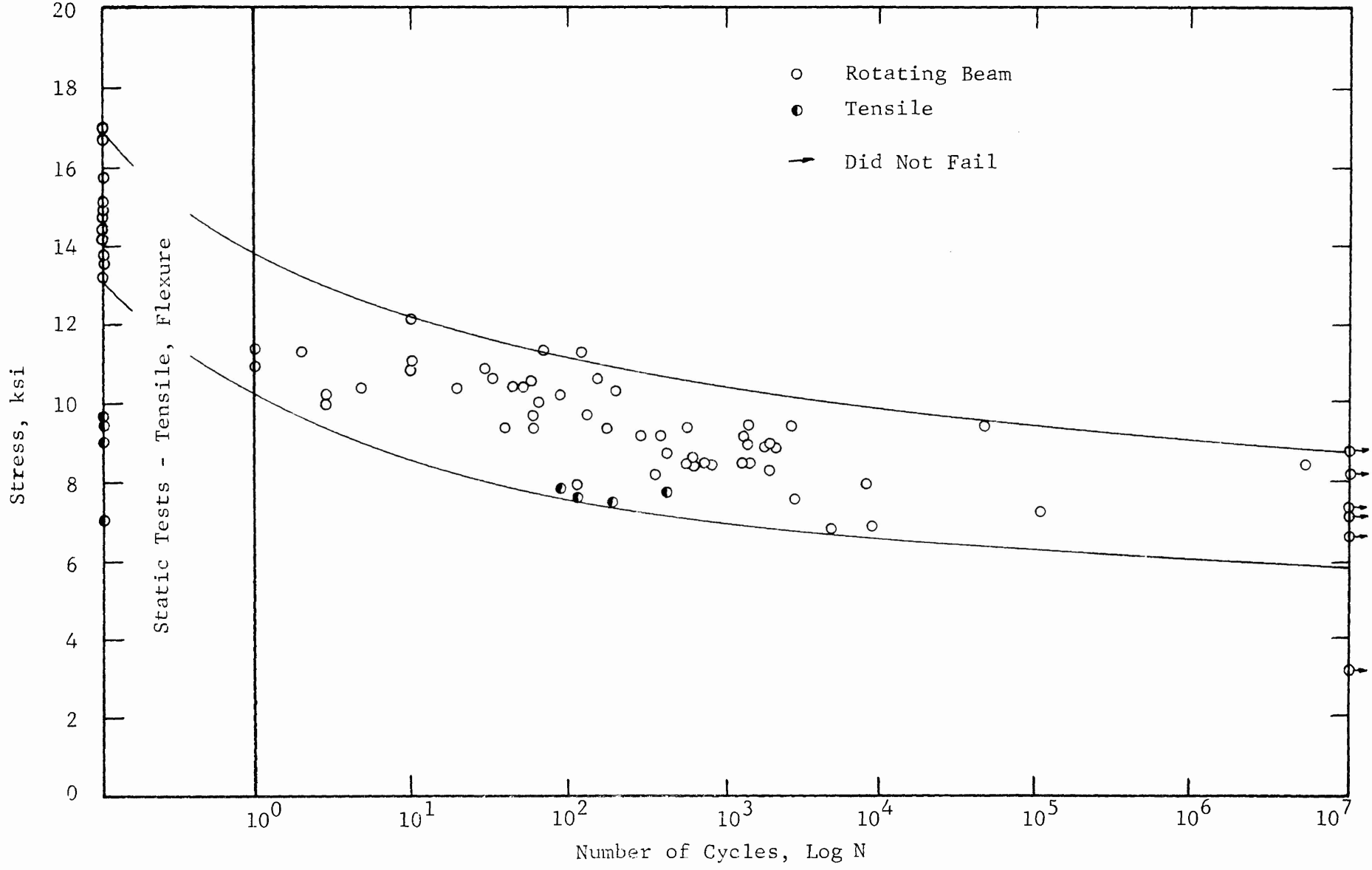


Figure 23. S-N CURVE FOR POCO-GRAPHITE (AXF-5Q) IN PURE TENSILE AND ROTATING BEAM CYCLIC FATIGUE

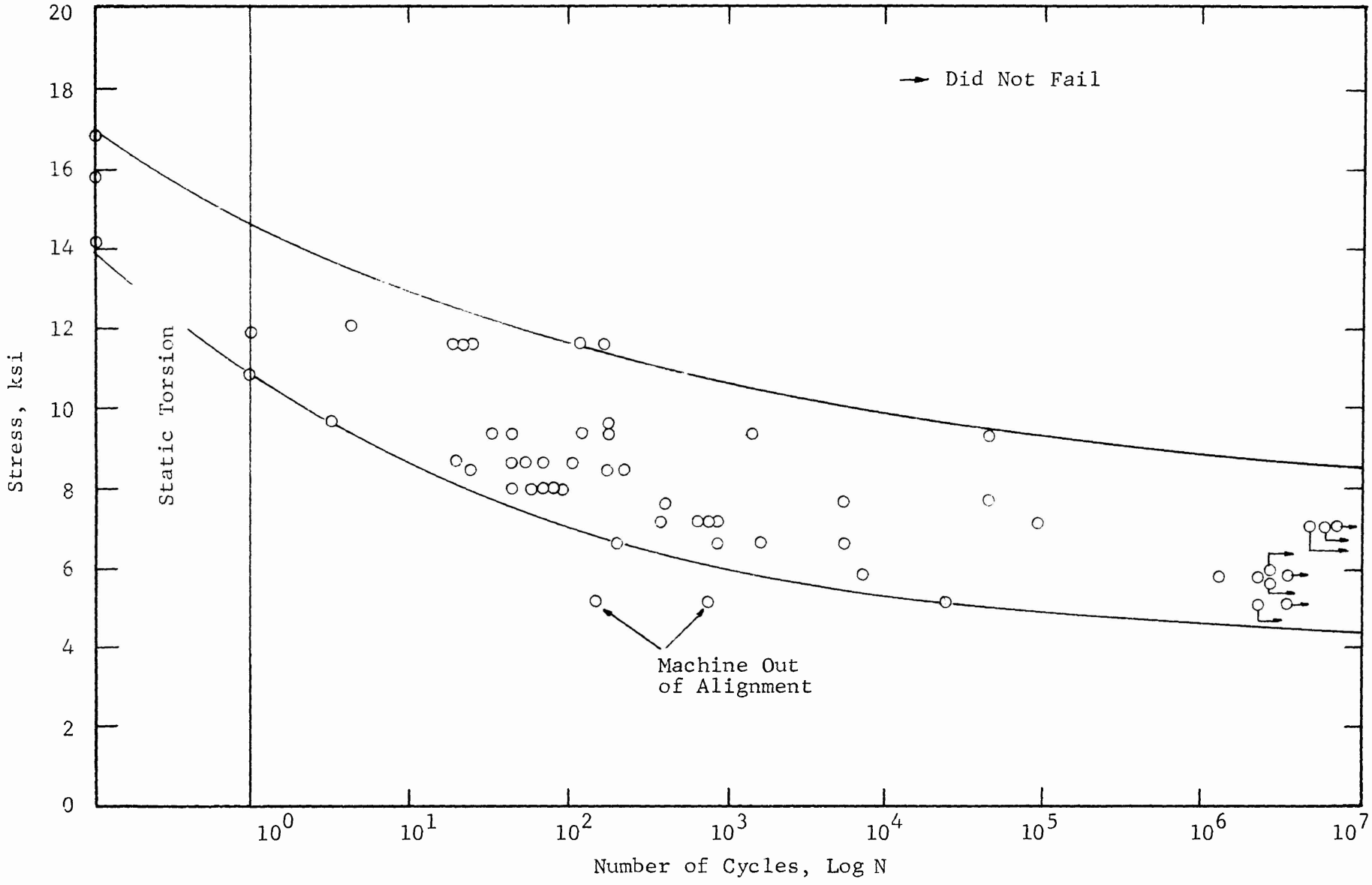


Figure 24. S-N CURVE FOR POCO-GRAPHITE (AXF-5Q) IN TORSIONAL FATIGUE

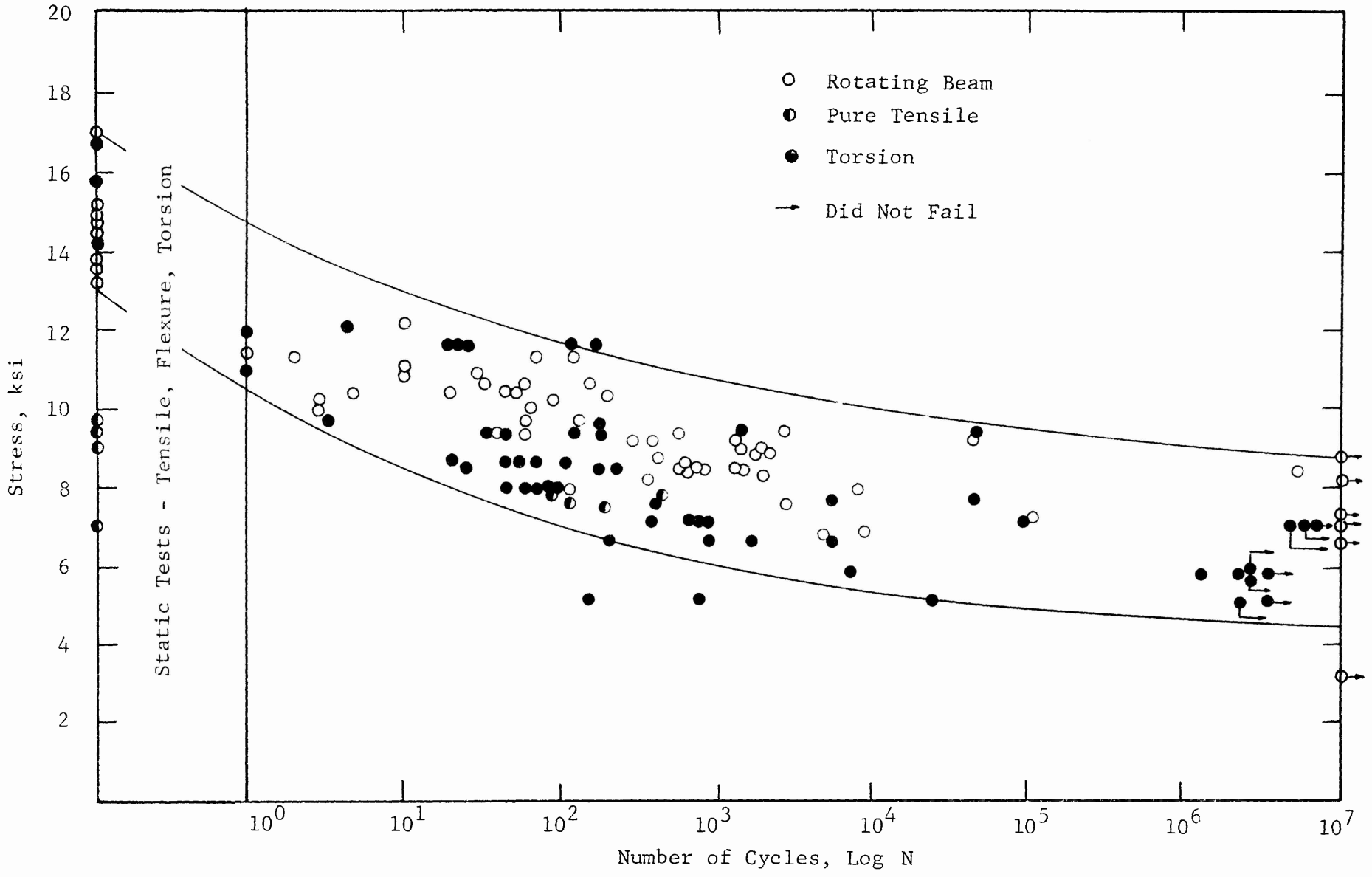


Figure 25. S-N CURVE FOR POCO-GRAPHITE (AXF-5Q) IN TENSILE, FLEXURAL AND TORSIONAL FATIGUE

in one S-N curve. With the exception of two values from the torsional fatigue data (machine was out of alignment), the results for both of the techniques used fell between the same upper and lower limits.

On this basis, it appears that variations in the material rather than techniques are responsible for the wide scatter in the data obtained from cyclic fatigue testing. This theory, however, should also be substantiated by other test techniques. One such test that should be included is flexural fatigue for simply supported beams on roller supports. Variations in shape of the specimen should also be considered so that shape/volume factors could be applied to strength criteria. Effects of depth to span ratio should be a factor that requires investigation as well as depth to thickness of the member.

## C. Results of Energy for Crack Initiation and Propagation Tests

The results of these tests are summarized in Table VIII. Typical fractures of the specimens, including pictures of initial cracking and propagation to failure of cracking for a double cantilever beam are shown in Figures 26 and 27.

### 1. Double Cantilever Beams

The data obtained from these tests, for both the V-grooved and the square-grooved notched specimens were in reasonably good agreement. For these tests the results were divided into two parts, the energy required to initiate the crack and the energy required to propagate the crack once it had been initiated.

Calculations of these energy values necessitated the use of the constant, n, described in Berry's[14] theoretical analysis. According to beam theory, this exponent should be about 3, but for these tests the value was slightly larger as shown in Figure 18, where the log value of the crack length is plotted against the log of the load-deflection ratio. The value was found to be valid for both V-notched and square notched specimens. It is clear from this figure that neither the slope nor the intercept of the best line through the experimental points agree with those expected from beam theory.

The average energy required to initiate cracking for the V-notched cantilevers was 3.305 in.-lb/in.$^2$, which was in good agreement with the value of 3.516 in.-lb/in.$^2$ for the square-notched specimens. However, it should be observed that the deviation in the data for the square-notched specimens was only 20%, whereas for the V-notched specimens the standard deviation was nearly 50%.

To account for this large deviation in the crack initiation energy exhibited by the V-notched specimens, it was

Table VIII

SUMMARY OF CRACK ENERGY TESTS FOR POCO-GRAPHITE (AXF-5Q)

| Test | Energy to initiate crack, in-lb/in$^2$ | Standard deviation in-lb/in$^2$ | Coefficient of variation, % | Energy of crack propagation in-lb/in$^2$ | Standard deviation in-lb/in$^2$ | Coefficient of variation, % |
|---|---|---|---|---|---|---|
| Double Cantilever, V-Groove | 3.305 | 1.780 | 48.0 | 3.238 | 0.447 | 12.0 |
| Double Cantilever, Square Groove | 3.516 | 0.733 | 20.0 | 2.715 | 0.152 | 5.6 |
| Four-Point Flexure, (Prenotched) | --- | --- | -- | 2.591 | 0.348 | 13.4 |

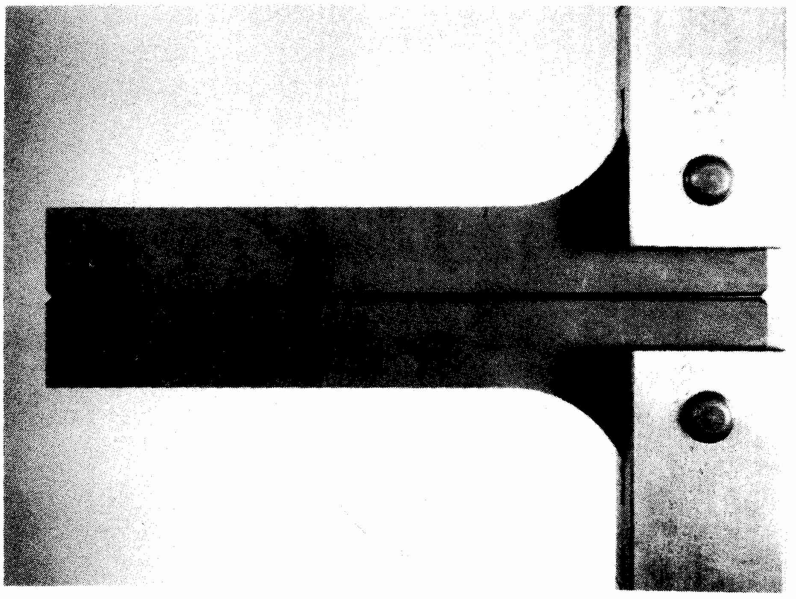

(a) First Cracking

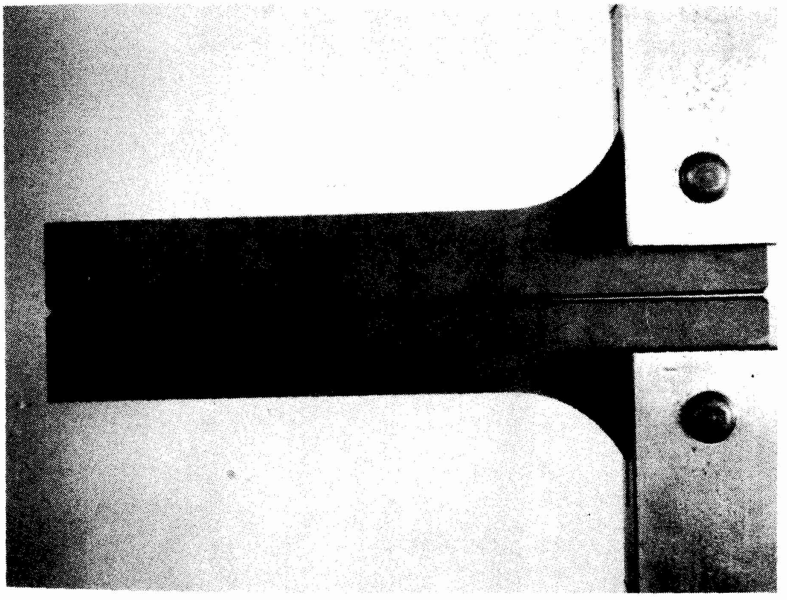

(b) Continued Cracking Under
Additional Load

Figure 26. DOUBLE CANTILEVER CRACK PROPAGATION TESTS ON POCO-GRAPHITE (AXF-5Q)

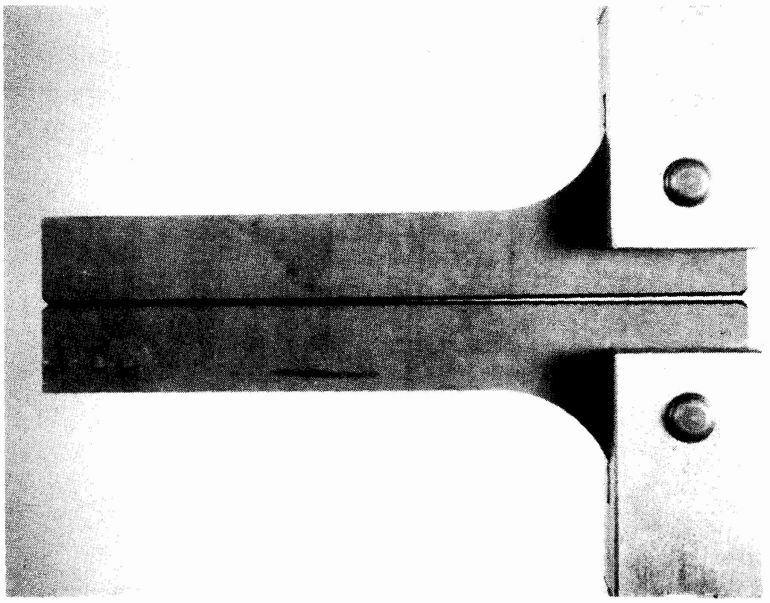

(c) Crack Extension
Under Further Load

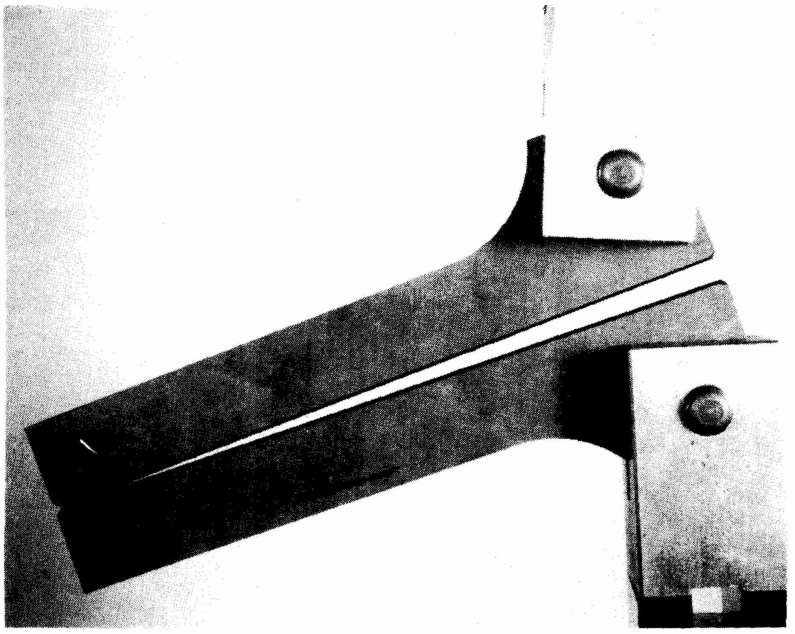

(d) Failure

Figure 27. DOUBLE CANTILEVER CRACK PROPAGATION TESTS ON POCO-GRAPHITE (AXF-5Q)

observed that the crack in the material did not always remain in the thinnest plane across the tip of the grooves. Because of this, it was occasionally difficult to trace the exact terminal point of the initial crack. It is therefore possible that for these specimens the initial crack was not as accurately measured as for the square-grooved specimens. In these latter specimens, the crack length was easier to determine because it never wandered out of the notched plane.

For crack propagation, the average energy required was 3.238 in.-lb/in.$^2$ for the V-notched specimens with a deviation of 12%. The crack propagation energy for the square-notched specimens was 2.715 in.-lb/in.$^2$ with a standard deviation of only 5.6%.

The values for both crack propagation and crack initiation are in fairly good agreement. Also, the fact that the load-deflection versus initial crack length data can be represented by the same straight line for both the V- and square-notched specimens leads one to believe that the scatter in the energy values can be accounted for by material variations rather than the testing technique used.

2. Flexural Tests for Crack Energy

Ten notched beams, tested in four-point flexure in the Instron testing machine gave the energy for cracking results shown in Table VIII. The average strain energy release rate for all 10 beams, computed from Eq. 28, was 2.591 in.-lb/in.$^2$ with a standard deviation of 0.31 in.-lb/in.$^2$ and a variation of 12%. A close inspection of the table shows that only one specimen, No. 8, failed at a considerably lower rate than the others. Examination of this specimen disclosed a flaw in the material at the tip of the pre-cut V-notch. As such, this one specimen could be considered invalid. If this one specimen is excluded from the analysis, the average fracture energy for the remaining nine specimens is 2.381 in.-lb/in.$^2$ with a deviation of 0.23 in.-lb/in.$^2$ and a variation of 7.9%. This value is only 10% less than the crack propagation energy value calculated for the square-notched double cantilever specimens.

Despite the slow rate of loading for these $\frac{1}{4}$ in. deep specimens, the fracture when it occurred was instantaneous and happened so fast that it was impossible to stop loading so that a new crack surface could be measured prior to the specimen breaking into two pieces. For this reason it is considered necessary to use deeper sections for future work in this type of crack-energy evaluation of brittle materials.

D. Biaxial Test Results

The results of the cylindrical biaxial tests are reported in Table IX and shown graphically in Figures 28 and 29.

Table IX

BIAXIAL TESTS ON POCO-GRAPHITE (AXF-5Q)
TENSION COMPRESSION STRESSES

| Specimen number | Vertical load, $P_v$, lb | $\sigma_v$ Comp. psi | Internal pressure $P_i$, lb/in$^2$ | Hoop stress $\sigma_t$, psi | Remarks |
|---|---|---|---|---|---|
| 1 | 530 | 1300 | 1400 | 9100 | Small vertical load only. Internal pressure to failure |
| 2 | 650 | 1592 | 1450 | 9425 | |
| 3 | 720 | 1764 | 1500 | 9750 | |
| 4 | 860 | 2100 | 1400 | 9100 | |
| 5 | 1224 | 3000 | 1350 | 8775 | Constant vertical load |
| 6 | 1428 | 3500 | 1325 | 8610 | Constant vertical load |
| 7 | 1428 | 3500 | 1300 | 8450 | Constant vertical load |
| 8 | 1428 | 3500 | 1450 | 9425 | Constant vertical load |
| 9 | 1632 | 4000 | 1400 | 9100 | Constant vertical load |
| 10 | 1632 | 4000 | 1200 | 7800 | Constant vertical load |
| 11 | 1632 | 4000 | 1100 | 7150 | Constant vertical load |
| 12 | 1836 | 4500 | 1350 | 8775 | Constant vertical load |
| 13 | 1836 | 4500 | 1400 | 9100 | Constant vertical load |
| 14 | 2040 | 5000 | 1450 | 9425 | Constant vertical load |
| 15 | 2040 | 5000 | 1400 | 9100 | Constant vertical load |

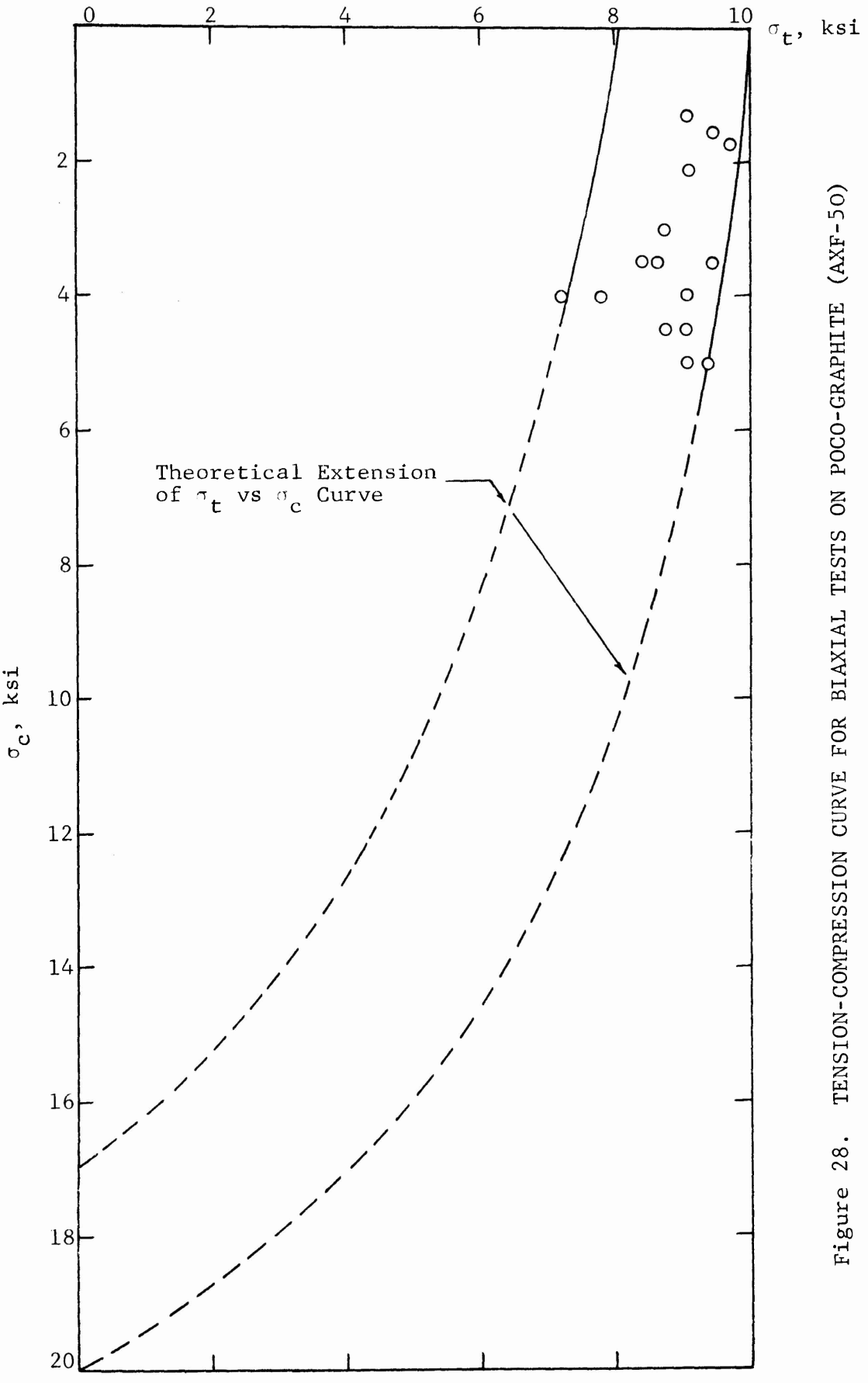


Figure 28. TENSION-COMPRESSION CURVE FOR BIAXIAL TESTS ON POCO-GRAPHITE (AXF-5Q)

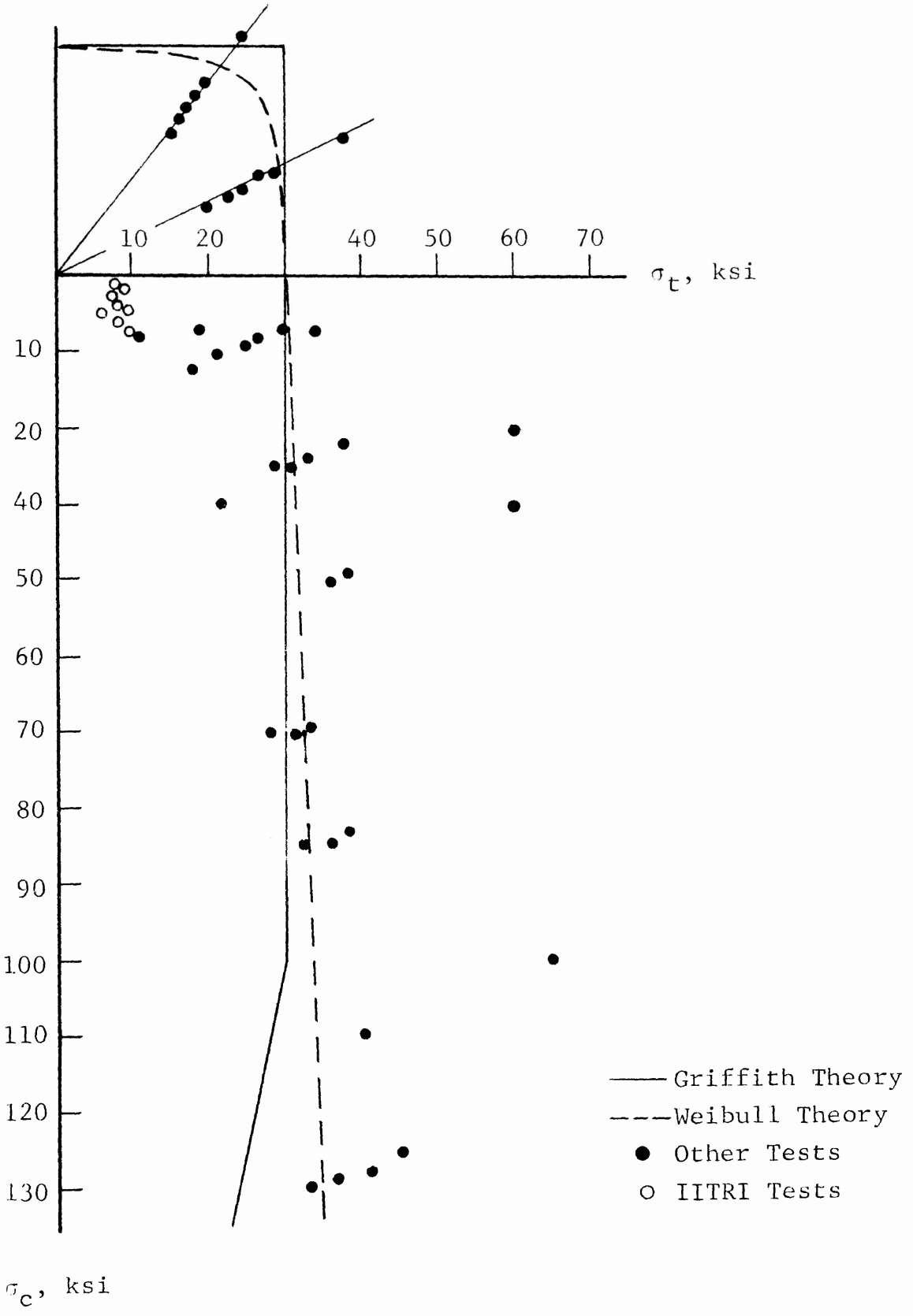


Figure 29. COMPARISON OF IITRI TESTS WITH THEORY

In view of all the tests described and reported herein, it was not surprising to find that there was a rather wide scatter in the results of the tests conducted on these specimens.

Although the number of specimens was relatively small and confined to low values of applied compressive stresses (between 1500 and 5000 psi) before introducing internal pressure for evaluating the hoop tensile stresses, the trend in the data is sufficient to indicate an upper and lower limit of combined axial stresses.

Compressive stresses were calculated from the known applied load and the area of the cylinder. Hoop stresses were calculated from:

$$\sigma_t = \frac{p_i r_i^2}{r_o^2 - r_i^2} \left(1 + \frac{r_o^2}{r^2}\right) \tag{31}$$

where $p_i$ = internal pressure, psi
$r_o$ = outer radius, in.
$r_i$ = inner radius, in.
and $\sigma_t$ is maximum for $r = r_i$.

For these simple hoop tension and tension-compression stresses, the ruptures were longitudinal cracks with minor side cracking. Similar ruptures were noted by Ely[19] for tension-compression biaxial stress tests on fine grained graphite tubular specimens.

## E. Conclusions and Recommendations

The conclusions drawn from these tests apply only to low toughness, low modulus, high strength brittle materials. The reason for this should be fairly obvious. In all of the tests, the results indicate that for any state of stress condition, or any manner of applying the loads the material exhibits upper and lower boundaries. This factor indicates that the low modulus materials are more sensitive to the effects of stress raisers such as notches, flaws or surface deformities. It is still felt, however, that the data is indicative of the test techniques for brittle material evaluation.

Of the methods used in evaluating the toughness of brittle materials, i.e., impact strength, it is thought that the drop weight test is least prone to error. The simplicity of the equipment used in this technique is a significant factor in this type of test. Any apparatus which, because of the component parts, is subject to machine losses which cannot be accurately

measured at all times and for each test should be avoided. The Charpy and Izod test equipment show varying resolutions for each type of head used and there appears to be no linear relationship between the kinetic energy values of the different heads. This makes the problem of evaluating the toughness of the material more complex. However, as a guide to establish a starting point for drop weight testing, the swinging pendulum tests give a good approximation of the impact energy to be expected.

It should be noted that the drop weight technique has not been established as valid for tests at elevated temperatures.

The results obtained from the static fatigue tests indicate that the techniques used produce good, valid evidence of the tensile and flexural fatigue properties of the material at room temperature. Perhaps the only test which requires further consideration is the static flexural fatigue. It has been stated that low modulus materials are more sensitive to surface effects than high modulus materials; therefore, further testing in this field should be considered. The effects of notches in static flexural fatigue should be evaluated. Because of the apparent influence of sustained loads on flexural specimens, and the fact that sustained tensile loads had no effect on the ultimate strength of the material, future work in this field should also include compressive static fatigue studies.

The cyclic fatigue data, while showing excellent correlation from the two techniques used should be substantiated by additional tests on specimens in three-point flexural fatigue. The reason for this is to study possible end effects. In both the rotating beam and the torsional fatigue, the ends of the specimens were gripped in chucks preventing end rotation or horizontal movement about the longitudinal axis. A flexural test would remove this restriction if the specimen was supported on rollers and would lead to an evaluation of end effects on fatigue properties.

The energy for fracture initiation and crack propagation require more intense study. The techniques used provide a good insight into the crack propagation energy of the material. However, certain refinements are required in future work. First, the double cantilevers should be saw-cut along the reduced horizontal plane from the end of the deepened section to the point of load application. The procedure would reduce the extent of the calculations and thereby reduce any chance of error. Second, the shape of these specimens should be revised. Rather than a radial change from the deepened section where the load is applied to the constant depth section of the specimen, it is suggested that future work should consider a linear gradual decrease in depth from the load point to the end of the cantilever.

In the case of the flexural tests for crack propagation, the flank angle and the depth of the preformed crack should be a variable under consideration. For such specimens one could then measure the spring constant for each beam prior to testing so that the analytical methods could be directly checked against the experimental work.

The results of the biaxial tests indicate that the techniques used provide useful information regarding multi-axial stress states for brittle materials. The key word to this phase is quantity. Many more tests on cylinders are necessary to validate the initial findings and these should be supported by tests in flat plates. In addition, the technique used should be adopted for investigating the effects of compression-compression as well as tension-tension states of stress.

The principal objection to extensive biaxial stress tests appears to be one of economy. The actual test itself is not too complex, but the preparation of the specimens is somewhat expensive. Since it is always essential to thicken the edges of these specimens to eliminate effects of load in the test area of the specimen, machining to these unusual shapes creates economic problems, the answer to which is yet to be found.

Insofar as the technique adopted is concerned, there appears to be only one small technicality to be overcome. That concerns the setting up to insure that perfect alignment between the specimen and the apparatus is made and maintained throughout the test.

Table X presents a summary of the recommended test procedures for determining the various strength and stress state parameters desired.

Table X

EVALUATION OF TESTS AND RECOMMENDED FUTURE TESTS

| Test | Rating | Application | Comments |
|---|---|---|---|
| Drop Weight | 1 | Impact | No machine losses to consider. |
| Charpy | 2 | Impact | Machine losses difficult to evaluate and not mathematically related. |
| Izod | 2 | Impact | |
| Double-Cantilever | 1 | Crack propagation | Use square-groove, precrack from free edge to load point. |
| Prenotched Beam | 1 | Crack propagation | Deeper section could be more effective. |
| Pin-loaded Beam | 1 | Tensile static fatigue | Straightforward test. |
| Three-point Flexure | 1 | Flexural static fatigue | Extend time to 100 hours. |
| Rotating-beam | 1 | Cyclic fatigue | Self-aligning technique. |
| Torsion | 2 | Cyclic fatigue | Alignment critical. |
| Cylinder | 1 | Biaxial | Extend tests to include; tension-tension; compression-compression. |

Table X (Cont'd)

EVALUATION OF TESTS AND RECOMMENDED FUTURE TESTS

| Test | Rating | Application | Comments |
|---|---|---|---|
| The Following Tests Are Recommended for Future Work. | | | |
| Four-point Flexure | | Flexural static fatigue | To substantiate three-point flexure findings. |
| Cylinder | | Compressive static fatigue | To support theory brought about by flexural static fatigue data. |
| Three-point Flexure | | Flexural cyclic fatigue | To add to the cyclic fatigue data already obtained. |
| Plate | | Biaxial | Tension-tension; tension-compression; compression-compression. |

REFERENCES


1. Griffith, A. A., Phil. Trans. Roy. Soc. 221A, London, pp. 163-198 (1920).

2. Cottrell, A. H., Fracture, John Wiley and Sons, New York (1959).

3. Irwin, G. R., Encyclopedia of Physics, Vol. VI, Springer Heidelberg (1958).

4. Davidenkov, N. H., Ed. Acad. Science, Moscow (1958).

5. Cottrell, A. H., "Structural Processes in Creep," Iron and Steel Inst., p. 1 (1961).

6. Davis, P. W., and Dutton, R., Acta Met., 14, 1138 (1966).

7. Cornet, I., and Gorum, A. E., Trans. AIME, 218-480 (1966).

8. Dally, J. W., "Design Data for Materials Employed in Thermal Protective System on Advanced Aerospace Vehicles," IIT Research Institute, ML-TDR-64-204, Vol. III (August 1965).

9. Polokowski, N. H., and Ripling, E., "Strength and Structure of Engineering Materials," 227-61, Prentice Hall, New Jersey (1966).

10. Salmassy, O. K., Duckworth, W. H., and Scharpe, A. D., "Behavior of Brittle State Materials," WADC Tech Rep. 53-5Q, Part I (June 1955).

11. Spath, W., Impact Testing of Materials, Gordon and Breach, New York (1961).

12. Tetelman, A. S., and McEvily, A. J., Fracture of Structural Materials, J. Wiley and Sons, New York (1967).

13. Bortz, S. A., and Wade, T. B., "Analysis of Mechanical Testing Procedure for Brittle Materials," IITRI for U. S. Army Materials Research Agency, Watertown, Massachusetts, AMRA CR 67-09/1 (1967).

14. Berry, J. P., "Determination of Fracture Surface Energies by the Cleavage Technique," Journal of Applied Physics, Vol. 34, No. 1 (January 1963).

15. Gillis, P. P., and Gilman, J. J., "Double Cantilever Mode of Crack Propagation," Journal of Applied Physics, Vol. 35 No. 1 (March 1964).

16. Corum, J. M., "Determination of Fracture Toughness of EGCR-Type Agot Graphite," Oak Ridge National Laboratory for U. S. Atomic Energy Commission, ORNL-4030 (December 1966).

17. Winne, D. H., and Wundt, B. M., "Application of the Griffith-Irwin Theory of Crack Propagation to the Bursting Behavior of Disks," Trans. ASME, Vol. 80, 1643-1658 (1958).

18. Ely, R. E., "Compressive Strength Behavior of a Fine-Grained Graphite as a Function of Specimen Geometry and Loading Rate," U. S. Army Missile Command, RR-TR-66-11 (July 1966).

19. Ely, R. E., "Strength of Magnesium Silicate and Graphite Under Biaxial Stress," Am. Ceram. Soc. Bull. Vol. 47, No. 5 (May 1968).

Appendix A

Table A-I

DROP WEIGHT TESTS

| Specimen number | Density (lb/in.$^3$) | Drop (in.) | Energy/Density (in.-lb/lb/in.$^3$) |
|---|---|---|---|
| 1 | .0675 | 19.82 | 18.17* |
| 2 | .0660 | 19.82 | 18.59* |
| 3 | .0656 | 19.82 | 18.71* |
| 4 | .0670 | 19.82 | 18.31* |
| 5 | .0670 | 19.82 | 18.31* |
| 6 | .0643 | 19.82 | 19.08* |
| 7 | .0670 | 19.82 | 18.31* |
| 8 | .0665 | 19.82 | 18.45* |
| 9 | .0663 | 19.82 | 18.50* |
| 10 | .0659 | 19.82 | 18.60* |
| 11 | .0636 | 20.02 | 19.48* |
| 12 | .0665 | 20.02 | 18.63* |
| 13 | .0663 | 20.02 | 18.69* |
| 14 | .0662 | 20.02 | 18.71* |
| 15 | .0659 | 20.22 | 19.00 |
| 16 | .0647 | 20.22 | 19.35 |
| 17 | .0662 | 20.41 | 19.08 |
| 18 | .0650 | 20.61 | 19.63* |
| 19 | .0659 | 20.61 | 19.36 |
| 20 | .0658 | 20.81 | 19.57* |
| 21 | .0673 | 20.81 | 19.14* |
| 22 | .0653 | 20.81 | 19.65 |
| 23 | .0669 | 21.00 | 19.43* |
| 24 | .0657 | 21.00 | 19.78 |
| 25 | .0663 | 21.00 | 19.60* |
| 26 | .0668 | 21.00 | 19.46 |
| 27 | .0668 | 21.00 | 19.46* |
| 28 | .0643 | 21.00 | 20.21* |
| 29 | .0661 | 21.00 | 19.66 |
| 30 | .0658 | 21.00 | 19.75 |
| 31 | .0692 | 21.00 | 18.79 |
| 32 | .0670 | 21.00 | 19.40 |
| 33 | .0670 | 21.00 | 19.40* |
| 34 | .0657 | 21.00 | 19.79* |
| 35 | .0660 | 21.00 | 19.69* |
| 36 | .0669 | 21.00 | 19.43* |
| 37 | .0654 | 21.16 | 20.03* |
| 38 | .0654 | 21.16 | 20.03* |
| 39 | .0651 | 21.16 | 20.12* |
| 40 | .0654 | 21.16 | 20.03* |
| 41 | .0654 | 21.16 | 20.03* |
| 42 | .0657 | 21.16 | 19.94 |

Table A-I (Cont'd)

DROP WEIGHT TESTS

| Specimen number | Density ($lb/in.^3$) | Drop (in.) | Energy/Density (in.-lb/$lb/in.^3$) |
|---|---|---|---|
| 43 | .0653 | 21.16 | 20.06* |
| 44 | .0657 | 21.16 | 19.94* |
| 45 | .0659 | 21.16 | 19.87* |
| 46 | .0657 | 21.16 | 19.94* |
| 47 | .0642 | 21.16 | 20.40 |
| 48 | .0652 | 21.16 | 20.09 |
| 49 | .0648 | 21.16 | 20.22* |
| 50 | .0653 | 21.16 | 20.06* |
| 51 | .0653 | 21.16 | 20.06* |
| 52 | .0652 | 21.16 | 20.09* |
| 53 | .0655 | 21.16 | 20.00 |
| 54 | .0657 | 21.18 | 19.95* |
| 55 | .0655 | 21.18 | 20.01 |
| 56 | .0657 | 21.18 | 19.95 |
| 57 | .0653 | 21.18 | 20.07* |
| 58 | .0644 | 21.18 | 20.36* |
| 59 | .0643 | 21.20 | 20.41* |
| 60 | .0665 | 21.20 | 19.73* |
| 61 | .0656 | 21.20 | 20.00* |
| 62 | .0670 | 21.20 | 19.58* |
| 63 | .0639 | 21.20 | 20.54 |
| 64 | .0663 | 21.20 | 19.79* |
| 65 | .0659 | 21.20 | 19.91* |
| 66 | .0660 | 21.20 | 19.88 |
| 67 | .0664 | 21.20 | 19.76* |
| 68 | .0651 | 21.20 | 20.16 |
| 69 | .0652 | 21.20 | 20.13 |
| 70 | .0668 | 21.20 | 19.64* |
| 71 | .0655 | 21.30 | 20.13* |
| 72 | .0652 | 21.30 | 20.22* |
| 73 | .0652 | 21.30 | 20.22* |
| 74 | .0654 | 21.30 | 20.16* |
| 75 | .0657 | 21.30 | 20.07* |
| 76 | .0651 | 21.30 | 20.25* |
| 77 | .0651 | 21.30 | 20.25* |
| 78 | .0655 | 21.30 | 20.13* |
| 79 | .0656 | 21.30 | 20.10* |
| 80 | .0654 | 21.30 | 20.16 |
| 81 | .0654 | 21.30 | 20.16 |
| 82 | .0657 | 21.30 | 20.07 |
| 83 | .0658 | 21.30 | 20.04* |
| 84 | .0657 | 21.30 | 20.07* |

Table A-I (Cont'd)

DROP WEIGHT TESTS

| Specimen number | Density ($lb/in.^3$) | Drop (in.) | Energy/Density (in.-lb/$lb/in.^3$) |
|---|---|---|---|
| 85 | .0655 | 21.30 | 20.13 |
| 86 | .0652 | 21.36 | 20.28 |
| 87 | .0657 | 21.36 | 20.12* |
| 88 | .0653 | 21.36 | 20.25 |
| 89 | .0654 | 21.36 | 20.22 |
| 90 | .0653 | 21.36 | 20.25* |
| 91 | .0665 | 21.40 | 19.92* |
| 92 | .0666 | 21.40 | 19.89 |
| 93 | .0668 | 21.40 | 19.83* |
| 94 | .0646 | 21.40 | 20.50 |
| 95 | .0666 | 21.40 | 19.89* |
| 96 | .0665 | 21.40 | 19.92* |
| 97 | .0660 | 21.40 | 20.07 |
| 98 | .0646 | 21.40 | 20.50 |
| 99 | .0661 | 21.40 | 20.04* |
| 100 | .0650 | 21.40 | 20.38 |
| 101 | .0654 | 21.44 | 20.29 |
| 102 | .0657 | 21.44 | 20.20* |
| 103 | .0653 | 21.44 | 20.32 |
| 104 | .0647 | 21.44 | 20.51* |
| 105 | .0656 | 21.44 | 20.23* |
| 106 | .0658 | 21.60 | 20.32 |
| 107 | .0653 | 21.60 | 20.48 |
| 108 | .0656 | 21.60 | 20.38* |
| 109 | .0651 | 21.44 | 20.39 |
| 110 | .0654 | 21.44 | 20.29* |
| 111 | .0650 | 21.44 | 20.42* |
| 112 | .0653 | 21.44 | 20.32* |
| 113 | .0652 | 21.44 | 20.36 |
| 114 | .0653 | 21.44 | 20.32* |
| 115 | .0654 | 21.44 | 20.29 |
| 116 | .0657 | 21.44 | 20.20 |
| 117 | .0659 | 21.44 | 20.14* |
| 118 | .0653 | 21.44 | 20.32* |
| 119 | .0645 | 21.44 | 20.57* |
| 120 | .0657 | 21.44 | 20.20 |
| 121 | .0650 | 21.44 | 20.42* |
| 122 | .0653 | 21.44 | 20.32 |
| 123 | .0662 | 21.44 | 20.05* |
| 124 | .0655 | 21.58 | 20.39 |
| 125 | .0648 | 21.58 | 20.61 |
| 126 | .0643 | 21.58 | 20.77* |

Table A-I (Cont'd)

DROP WEIGHT TESTS

| Specimen number | Density ($lb/in.^3$) | Drop (in.) | Energy/Density ($in.-lb/lb/in.^3$) |
|---|---|---|---|
| 127 | .0650 | 21.58 | 20.55* |
| 128 | .0649 | 21.58 | 20.58 |
| 129 | .0660 | 21.58 | 20.24* |
| 130 | .0655 | 21.58 | 20.39* |
| 131 | .0642 | 21.58 | 20.81* |
| 132 | .0659 | 21.58 | 20.27* |
| 133 | .0665 | 21.58 | 20.09 |
| 134 | .0663 | 21.58 | 20.15 |
| 135 | .0649 | 21.58 | 20.58 |
| 136 | .0650 | 21.58 | 20.55* |
| 137 | .0657 | 21.58 | 20.33* |
| 138 | .0650 | 21.58 | 20.36* |
| 139 | .0656 | 21.60 | 20.38 |
| 140 | .0649 | 21.60 | 20.60 |
| 141 | .0653 | 21.60 | 20.48 |
| 142 | .0665 | 21.60 | 20.10 |
| 143 | .0668 | 21.60 | 20.01* |
| 144 | .0667 | 21.60 | 20.04 |
| 145 | .0652 | 21.60 | 20.50* |
| 146 | .0656 | 21.60 | 20.38 |
| 147 | .0668 | 21.60 | 20.01* |
| 148 | .0668 | 21.60 | 20.01* |
| 149 | .0652 | 21.60 | 20.50 |
| 150 | .0665 | 21.60 | 20.10* |
| 151 | .0639 | 21.71 | 21.03 |
| 152 | .0659 | 21.71 | 20.39 |
| 153 | .0646 | 21.71 | 20.80* |
| 154 | .0656 | 21.71 | 20.48 |
| 155 | .0658 | 21.71 | 20.42* |
| 156 | .0655 | 21.71 | 20.51 |
| 157 | .0651 | 21.71 | 20.64 |
| 158 | .0656 | 21.71 | 20.48* |
| 159 | .0647 | 21.71 | 20.77 |
| 160 | .0654 | 21.71 | 20.55 |
| 161 | .0653 | 21.71 | 20.58* |
| 162 | .0653 | 21.71 | 20.58* |
| 163 | .0648 | 21.71 | 20.74* |
| 164 | .0648 | 21.71 | 20.74 |
| 165 | .0654 | 21.71 | 20.55 |
| 166 | .0666 | 21.79 | 20.25 |
| 167 | .0648 | 21.79 | 20.81* |
| 168 | .0686 | 21.79 | 19.66* |

Table A-I (Cont'd)

DROP WEIGHT TESTS

| Specimen number | Density ($lb/in.^3$) | Drop (in.) | Energy/Density (in.-lb/$lb/in.^3$) |
|---|---|---|---|
| 169 | .0664 | 21.79 | 20.31* |
| 170 | .0661 | 21.79 | 20.41 |
| 171 | .0681 | 21.79 | 19.80 |
| 172 | .0621 | 21.79 | 21.72 |
| 173 | .0661 | 21.79 | 20.40 |
| 174 | .0665 | 21.79 | 20.28* |
| 175 | .0652 | 21.79 | 20.69 |
| 176 | .0655 | 21.83 | 20.63* |
| 177 | .0652 | 21.83 | 20.72 |
| 178 | .0656 | 21.83 | 20.60 |
| 179 | .0657 | 21.83 | 20.57 |
| 180 | .0658 | 21.83 | 20.53 |
| 181 | .0649 | 21.85 | 20.84 |
| 182 | .0655 | 21.85 | 20.65* |
| 183 | .0657 | 21.85 | 20.59 |
| 184 | .0652 | 21.85 | 20.74* |
| 185 | .0658 | 21.85 | 20.56* |
| 186 | .0653 | 21.85 | 20.71* |
| 187 | .0645 | 21.85 | 20.97 |
| 188 | .0659 | 21.85 | 20.52 |
| 189 | .0653 | 21.85 | 20.71 |
| 190 | .0652 | 21.85 | 20.74 |
| 191 | .0658 | 21.85 | 20.56 |
| 192 | .0657 | 21.85 | 20.59* |
| 193 | .0656 | 21.85 | 20.62* |
| 194 | .0652 | 21.85 | 20.74 |
| 195 | .0658 | 21.85 | 20.56* |
| 196 | .0664 | 21.90 | 20.50* |
| 197 | .0654 | 21.99 | 20.81 |
| 198 | .0655 | 21.99 | 20.78 |
| 199 | .0654 | 21.99 | 20.81 |
| 200 | .0653 | 21.99 | 20.84 |
| 201 | .0675 | 21.99 | 20.17* |
| 202 | .0658 | 21.99 | 20.68 |
| 203 | .0654 | 21.99 | 20.81* |
| 204 | .0657 | 21.99 | 20.72 |
| 205 | .0657 | 21.99 | 20.72* |
| 206 | .0651 | 21.99 | 20.91 |
| 207 | .0656 | 21.99 | 20.75 |
| 208 | .0646 | 21.99 | 21.07 |
| 209 | .0668 | 21.99 | 20.38 |
| 210 | .0650 | 21.99 | 20.94 |

Table A-I (Cont'd)

DROP WEIGHT TESTS

| Specimen number | Density ($lb/in.^3$) | Drop (in.) | Energy/Density ($in.-lb/lb/in.^3$) |
|---|---|---|---|
| 211 | .0665 | 21.99 | 20.47 |
| 212 | .0664 | 21.99 | 20.50 |
| 213 | .0644 | 21.99 | 21.13 |
| 214 | .0659 | 21.99 | 20.65* |
| 215 | .0642 | 21.99 | 21.20 |
| 216 | .0668 | 21.99 | 20.38 |
| 217 | .0659 | 21.99 | 20.65 |
| 218 | .0667 | 21.99 | 20.41 |
| 219 | .0656 | 22.13 | 20.88* |
| 220 | .0653 | 22.13 | 20.98 |
| 221 | .0654 | 22.13 | 20.95* |
| 222 | .0655 | 22.13 | 20.92 |
| 223 | .0657 | 22.13 | 20.85 |
| 224 | .0655 | 22.13 | 20.92* |
| 225 | .0654 | 22.13 | 20.95 |
| 226 | .0649 | 22.13 | 21.11 |
| 227 | .0651 | 22.13 | 21.05 |
| 228 | .0652 | 22.13 | 21.01 |
| 229 | .0670 | 22.19 | 20.50* |
| 230 | .0671 | 22.19 | 20.47 |
| 231 | .0667 | 22.19 | 20.59* |
| 232 | .0660 | 22.19 | 20.81 |
| 233 | .0652 | 22.19 | 21.06 |
| 234 | .0651 | 22.19 | 21.10 |
| 235 | .0664 | 22.19 | 20.60 |
| 236 | .0661 | 22.19 | 20.78 |
| 237 | .0645 | 22.19 | 21.29 |
| 238 | .0642 | 22.19 | 21.39 |
| 239 | .0655 | 22.21 | 20.99 |
| 240 | .0655 | 22.21 | 20.99* |
| 241 | .0655 | 22.21 | 20.99 |
| 242 | .0654 | 22.21 | 21.02 |
| 243 | .0652 | 22.21 | 21.09* |
| 244 | .0652 | 22.21 | 21.09 |
| 245 | .0644 | 22.21 | 21.35 |
| 246 | .0651 | 22.21 | 21.12 |
| 247 | .0655 | 22.21 | 20.99 |
| 248 | .0658 | 22.21 | 20.90 |
| 249 | .0653 | 22.21 | 21.06* |
| 250 | .0654 | 22.21 | 21.02 |
| 251 | .0657 | 22.21 | 20.93 |
| 252 | .0653 | 22.21 | 21.06 |

Table A-I (Cont'd)

DROP WEIGHT TESTS

| Specimen number | Density ($lb/in.^3$) | Drop (in.) | Energy/Density ($in.-lb/lb/in.^3$) |
|---|---|---|---|
| 253 | .0658 | 22.21 | 20.90 |
| 254 | .0667 | 22.38 | 20.77* |
| 255 | .0668 | 22.38 | 20.74* |
| 256 | .0660 | 22.38 | 20.99* |
| 257 | .0667 | 22.38 | 20.77 |
| 258 | .0666 | 22.38 | 20.81 |
| 259 | .0653 | 22.38 | 21.21 |
| 260 | .0643 | 22.38 | 21.55* |
| 261 | .0666 | 22.38 | 20.80* |
| 262 | .0646 | 22.38 | 21.46 |
| 263 | .0652 | 22.38 | 21.25 |
| 264 | .0650 | 22.60 | 21.54 |
| 265 | .0652 | 22.60 | 21.47 |
| 266 | .0655 | 22.60 | 21.37 |
| 267 | .0647 | 22.60 | 21.64 |
| 268 | .0661 | 22.60 | 21.18* |
| 269 | .0660 | 22.60 | 21.21 |
| 270 | .0666 | 22.60 | 21.62 |
| 271 | .0668 | 22.60 | 20.95 |
| 272 | .0658 | 22.60 | 21.27 |
| 273 | .0652 | 22.60 | 21.47 |
| 274 | .0656 | 22.97 | 21.68 |
| 275 | .0649 | 22.97 | 21.91 |
| 276 | .0677 | 22.97 | 21.00 |
| 277 | .0665 | 22.97 | 21.39 |
| 278 | .0670 | 22.97 | 21.22 |
| 279 | .0657 | 22.97 | 21.64 |
| 280 | .0669 | 22.97 | 21.25 |
| 281 | .0666 | 22.97 | 21.35 |
| 282 | .0669 | 22.97 | 21.26* |
| 283 | .0653 | 22.97 | 21.77* |
| 284 | .0654 | 23.37 | 22.12 |
| 285 | .0669 | 23.37 | 21.63* |
| 286 | .0667 | 23.76 | 22.05 |
| 287 | .0666 | 23.76 | 22.08 |
| 288 | .0641 | 23.76 | 22.90 |
| 289 | .0669 | 23.76 | 21.99 |
| 290 | .0647 | 23.76 | 22.73 |
| 291 | .0671 | 23.76 | 21.90 |
| 292 | .0666 | 23.76 | 22.08 |
| 293 | .0670 | 23.76 | 21.95 |
| 294 | .0660 | 23.76 | 22.28 |
| 295 | .0673 | 23.76 | 21.85 |
| 296 | .0672 | 23.76 | 21.80 |

*Did not fail.

Table A-II

SUMMARY OF DROP WEIGHT IMPACT TESTS
ON POCO-GRAPHITE (AXF-5Q)

| Drop (in.) | Number of specimens | Energy range (in.-lb)* | Percent failed |
|---|---|---|---|
| 23.00 to 24.00 | 12 | 1.42 to 1.49 | 100 |
| 22.50 to 22.99 | 31 | 1.39 to 1.42 | 80 |
| 22.00 to 22.49 | 35 | 1.36 to 1.39 | 72 |
| 21.50 to 21.99 | 98 | 1.33 to 1.36 | 58 |
| 21.00 to 21.49 | 84 | 1.30 to 1.33 | 35 |
| 20.00 to 20.99 | 26 | 1.24 to 1.30 | 21 |
| Less than 19.99 | 10 | 1.23 | 0 |

*Energy range selected as criteria of probability of failure to allow for variations in material density.

Weight of Steel Ball = 0.0619 lb
Mean Weighted Average = 1.388 in.-lb
Standard Deviation = 0.062 in.-lb
Coefficient of Variance = 4.5%

Table A-III

REPEATED IMPACT TESTS
ON POCO-GRAPHITE (AXF-5Q)

| Test | Specimen number | Energy (in.-lb) | Number of strikes |
|---|---|---|---|
| Drop-Weight | 2 | 1.258 | 5 |
| | 3 | 1.266 | 4 |
| | 5 | 1.239 | 3 |
| | 8 | 1.249 | 5 |
| | 10 | 1.259 | 3 |
| | 72 | 1.368 | 4 |
| | 74 | 1.365 | 5 |
| | 77 | 1.371 | 1 |
| | 78 | 1.363 | 2 |
| | 84 | 1.359 | 4 |
| | 117 | 1.363 | 3 |
| | 119 | 1.393 | 4 |
| | 121 | 1.382 | 2 |
| | 123 | 1.357 | 5 |
| | 127 | 1.391 | 1 |
| | 131 | 1.409 | 2 |
| | 158 | 1.386 | 1 |
| | 162 | 1.393 | 1 |
| | 184 | 1.404 | 2 |
| | 193 | 1.396 | 1 |
| Izod-Unnotched | B 4 | 1.504 | 9 |
| | B 5 | 1.605 | 11 |
| | B 6 | 1.537 | 10 |
| | B 7 | 1.453 | 8 |
| | B 8 | 1.453 | 8 |
| | B 9 | 1.504 | 9 |
| | B 10 | 1.402 | 7 |
| | B 11 | 1.335 | 6 |
| | B 12 | 1.605 | 11 |
| | B 13 | 1.504 | 9 |
| Charpy-Unnotched | B 14 | 1.378 | 11 |
| | B 15 | 1.345 | 10 |
| | B 16 | 1.280 | 9 |
| | B 17 | 1.345 | 10 |
| | B 18 | 1.280 | 9 |
| | B 19 | 1.441 | 10 |
| | B 20 | 1.345 | 12 |
| | B 21 | 1.217 | 8 |
| | B 22 | 1.506 | 13 |
| | B 23 | 1.345 | 10 |

Table A-III

REPEATED IMPACT TESTS
ON POCO-GRAPHITE (AXF-5Q)

| Test | Specimen number | Energy (in.-lb) | Number of strikes |
|---|---|---|---|
| Izod-Notched | 144 | 0.456 | 11 |
| | 145 | 0.370 | 9 |
| | 146 | 0.456 | 11 |
| | 147 | 0.456 | 11 |
| | 148 | 0.422 | 10 |
| | 149 | 0.456 | 11 |
| | 150 | 0.558 | 13 |
| | 151 | 0.507 | 12 |
| | 152 | 0.370 | 9 |
| | 153 | 0.456 | 11 |
| Charpy-Notched | 154 | 0.320 | 10 |
| | 155 | 0.270 | 7 |
| | 156 | 0.270 | 7 |
| | 157 | 0.304 | 9 |
| | 158 | 0.304 | 9 |
| | 159 | 0.288 | 8 |
| | 160 | 0.270 | 7 |
| | 161 | 0.288 | 8 |
| | 162 | 0.288 | 8 |
| | 163 | 0.270 | 7 |

Table A-IV

ENERGY FOR CRACK PROPAGATION
FOR POCO-GRAPHITE (AXF-5Q) BY CLEAVAGE

| Specimen number* | P** (lb) | Δ (in.) | G1*** (in.-lb/in.$^2$) | G2*** (in.-lb/in.$^2$) |
|---|---|---|---|---|
| V1 | 208 | .085 | 1.421 | 3.908 |
| V2 | 420 | .035 | 5.160 | 2.415 |
| V3 | 468 | .033 | 7.680 | 3.197 |
| V4 | 275 | .121 | 2.220 | 2.720 |
| V5 | 296 | .083 | 2.207 | 3.028 |
| V6 | 258 | .151 | 2.337 | 4.185 |
| V7 | 326 | .082 | 2.000 | 3.219 |
| S8 | 355 | .109 | 4.100 | 2.353 |
| S9 | 334 | .060 | 3.160 | 2.674 |
| S10 | 336 | .184 | 3.930 | 2.536 |
| S11 | 312 | .180 | 3.020 | 2.767 |
| S12 | 377 | .246 | 4.220 | --- |
| S13 | 406 | .364 | 5.217 | --- |
| S14 | 298 | .109 | 2.681 | 2.787 |
| S15 | 301 | .092 | 2.691 | 2.826 |
| S16 | 306 | .139 | 2.626 | 3.062 |

*V = V-Groove; S = Square Groove

**Total load to initiate crack.

***G1 = Energy for crack initiation.
G2 = energy for crack propagation.

Table A-V

ENERGY FOR CRACK PROPAGATION
FOR POCO-GRAPHITE (AXF-5Q)
BY FOUR-POINT FLEXURE TESTS

| Specimen number | P (lb) | $\Delta$ (in.) | $\sigma_n$ (psi) | G (in.-lb/in.$^2$) |
|---|---|---|---|---|
| 1 | 30.00 | .0155 | 7720 | 2.375 |
| 2 | 32.50 | .0145 | 8360 | 2.781 |
| 3 | 30.00 | .0145 | 7720 | 2.375 |
| 4 | 34.00 | .0165 | 8750 | 3.048 |
| 5 | 32.50 | .0160 | 8360 | 2.781 |
| 6 | 32.00 | .0143 | 8230 | 2.698 |
| 7 | 34.00 | .0165 | 8750 | 3.048 |
| 8 | 25.00 | .0155 | 6430 | 1.645* |
| 9 | 32.50 | .0150 | 8360 | 2.781 |
| 10 | 30.00 | .0147 | 7720 | 2.375 |

*Flaw at tip of notch.

DISTRIBUTION LIST

Contract DA-19-066-AMC-321(X)

"Analysis and Review of Mechanical Testing Procedures for Brittle Materials"

| No. of Copies | To |
|---|---|
| 1 | Office of the Director, Defense Research and Engineering, The Pentagon, Washington, D. C. 20301 |
| 20 | Commander, Defense Documentation Center, Cameron Station, Building 5, 5010 Duke Street, Alexandria, Virginia 22314 |
| 1 | Defense Metals Information Center, Battelle Memorial Institute, Columbus, Ohio 43201 |
| | Chief of Research and Development, Department of the Army, Washington, D. C. 20310 |
| 2 | ATTN: Physical and Engineering Sciences Division |
| | Commanding Officer, Army Research Office (Durham), Box CM, Duke Station, Durham, North Carolina 27706 |
| 1 | ATTN: Information Processing Office |
| | Commanding General, U. S. Army Material Command, Washington, D. C. 20315 |
| 1 | ATTN: AMCRD-RC-M |
| | Commanding General, Deseret Test Center, Fort Douglas, Utah 84113 |
| 1 | ATTN: Technical Information Office |
| | Commanding General, U. S. Army Electronics Command, Fort Monmouth, New Jersey 07703 |
| 2 | ATTN: AMSEL-RD-MAT |
| | Commanding General, U. S. Army Missile Command, Redstone Arsenal, Alabama 35809 |
| 1 | ATTN: Technical Library |
| | Commanding General, U. S. Army Munitions Command, Dover, New Jersey 07801 |
| 1 | ATTN: Technical Library |
| | Commanding General, U. S. Army Natick Laboratories, Natick, Massachusetts, 01762 |
| 1 | ATTN: Technical Library |

Commanding General, U. S. Army Satellite Communications Agency, Fort Monmouth, New Jersey 07703
1 ATTN: Technical Document Center

Commanding General, U. S. Army Tank-Automotive Center, Warren, Michigan 48090
2 ATTN: SMOTA-RTS, Tech. Data Coord. Br.

Commanding General, U. S. Army Weapons Command, Research and Development Directorate, Rock Island, Illinois 61202
1 ATTN: AMSWE-RDR

Commanding Officer, Aberdeen Proving Ground, Maryland 21005
1 ATTN: Technical Library, Building 313

Commanding Officer, Frankford Arsenal, Bridge and Tacony Streets, Philadelphia, Pennsylvania 19137
1 ATTN: Library Branch C 2500

Commanding Officer, Harry Diamond Laboratories, Connecticut Avenue and Van Ness Street, N. W. Washington, D. C. 20438
1 ATTN: Technical Information Office

Commanding Officer, Department of the Army, Ohio River Division Laboratories, Corps of Engineers, 5158 Mariemont Avenue, Cincinnati, Ohio 45227
1 ATTN: ORDLB-TR

Commanding Officer, Picatinny Arsenal Dover, New Jersey 07801
1 ATTN; SMUPA-VA6

Commanding Officer, Redstone Scientific Information Center, U. S. Army Missile Command, Redstone Arsenal, Alabama 35809
4 ATTN: AMSMI-RBLD, Document Section

Commanding Officer, Watervliet Arsenal, Watervliet, New York 12189
1 ATTN: SWEWV-RDT, Technical Information Services Office

1 Commanding Officer, U. S. Army Aviation Material Laboratories, Fort Eustis, Virginia 23604

Commanding Officer, U. S. Army Aviation School Library, Fort Rucker, Alabama 36360
1 ATTN: USAAVNS-P&NRI

Commanding Officer, USACDC Ordnance Agency, Aberdeen Proving Ground, Maryland 21005
2 ATTN: Library, Building 305

Commanding Officer, U. S. Army Engineer Waterways Experiment Station, Vicksburg, Mississippi 39180
1 ATTN: Research Center Library

Director, Naval Research Laboratory, Anacostia Station, Washington, D. C. 30490
1 ATTN: Technical Information Officer

Chief, Office of Naval Research, Department of the Navy, Washington, D. C. 20315
1 ATTN: Code 423

Headquarters, Aeronautical Systems Division, Wright-Patterson Air Force Base, Ohio 45433
5 ATTN: ASRCEE

1 U. S. Atomic Energy Commission, Office of Technical Information Extension, P. O. Box 62, Oak Ridge, Tennessee 37830

National Aeronautics and Space Administration, Marshall Space Flight Center, Huntsville, Alabama 35812
1 ATTN: R-P&VE-M, Dr. W. R. Lucas
1 ATTN: M-F&AE-M, Mr. W. A. Wilson, Building 4720

National Aeronautics and Space Administration, Washington, D. C. 20546
1 ATTN: Mr. B. G. Achhammer
1 ATTN: Mr. G. C. Deutsch
1 ATTN: Mr. R. V. Rhode

1 Dr. T. Vasilos, Avco Corporation, Avco Space Systems Division, Research and Technology Laboratories, 201 Lowell Street, Wilmington, Massachusetts 01887

1 Professor Richard M. Spriggs, Associate Director, Materials Research Center and Associate Professor, Department of Metallurgical Engineering, Lehigh University, Bethlehem, Pennsylvania

1 Dr. N. M. Parikh, Director, Metals Research, IIT Research Institute, 10 West 35th Street, Chicago, Illinois 60616

1 S. A. Bortz, Senior Research Engineer, Ceramics Research, IIT Research Institute, 10 West 35th Street, Chicago, Illinois 60616

1 Professor V. Vand, The Pennsylvania State University, Materials Research Laboratory, University Park, Pennsylvania 16802

1 Dr. J. Pappis, Raytheon Company, Research Division, Waltham, Massachusetts 02154

Commanding Officer, U. S. Army Materials and Mechanics Research Center, Watertown, Massachusetts 02172
5 ATTN: AMXMR-AT
1 ATTN: AMXMR-AX
1 ATTN: AMXMR-RP
1 ATTN: AMXMR-RX

1 Dr. Sidney Ross, Pitman-Dunn Research Laboratories, SMUFA-L6000-64-4, Frankford Arsenal, Philadelphia, Pennsylvania 19137

1 Dr. William McNeill, Pitman-Dunn Research Laboratories, SMUFA-L8400, Frankford Arsenal, Philadelphia, Pennsylvania 19137

1 Dr. B. Steverding, U. S. Army Missile Command, Physical Sciences Laboratories, AMSMI-RR, Redstone Arsenal, Huntsville, Alabama

1 Dr. Morton I. Kliman, 215 Waverly Avenue, Newton, Massachusetts

1 Mr. Sam DiVita, U. S. Army Electronics Command, Electronic Parts & Materials Division, AMSEL-KL-EC, Fort Monmouth, New Jersey

1 Dr. C. W. H. Barnett, Harry Diamond Laboratories, Washington, D. C. 20438

1 Mr. P. E. Houser, Munitions Command, Picatinny Arsenal, Dover, New Jersey 07801

1 Mr. I. Pepper, Corps of Engineers, Waterways Experiment Station, Jackson, Mississippi 39180

1 Mr. Sol Bremmer, Douglas Aircraft, El Segundo, California 90245

UNCLASSIFIED
Security Classification

DOCUMENT CONTROL DATA - R&D
(Security classification of title, body of abstract and indexing annotation must be entered when the overall report is classified)

1. ORIGINATING ACTIVITY (Corporate author)
IIT Research Institute
Chicago, Illinois 60616

2a. REPORT SECURITY CLASSIFICATION
Unclassified

2b. GROUP

3. REPORT TITLE
Analysis and Review of Mechanical Testing Procedures for Brittle Materials

4. DESCRIPTIVE NOTES (Type of report and inclusive dates)
Final Report 16 March 1967 to 15 February 1968

5. AUTHOR(S) (Last name, first name, initial)
Bortz, Seymour A., and Burton, Kenneth T.

| 6. REPORT DATE | 7a. TOTAL NO. OF PAGES | 7b. NO. OF REFS |
|---|---|---|
| July 1968 | 96 | 19 |

| 8a. CONTRACT OR GRANT NO. | 9a. ORIGINATOR'S REPORT NUMBER(S) |
|---|---|
| DA-19-066-AMC-321(X) | AMRA CR 67-09(F) |
| b. PROJECT NO. D/A 1C024401A330 | 9b. OTHER REPORT NO(S) (Any other numbers that may be assigned this report) |
| c. AMCMS Code 5025.11.296 | |
| d. | |

10. AVAILABILITY/LIMITATION NOTICES
This document has been approved for public release and sale; its distribution is unlimited.

| 11. SUPPLEMENTARY NOTES | 12. SPONSORING MILITARY ACTIVITY |
|---|---|
| | Army Materials and Mechanics Research Center<br>Watertown, Massachusetts 02172 |

13. ABSTRACT

The purpose of this research is to provide a guide for investigators in the performance of mechanical tests and the interpretation of test results. A review of the philosophy of testing and the problem areas in studying brittle materials is provided.

Research effort consists of investigating mechanical test procedures and analyzing property data with regard to these test procedures, so that the best practice can be determined. Evaluated information is organized into three sections:

1. Test philosophy, test techniques and analytical methods
2. Correlation of laboratory tests and recommended procedures
3. Tabular presentation of test data

DD FORM 1 JAN 64 1473

UNCLASSIFIED
Security Classification

| 14. KEY WORDS | LINK A | | LINK B | | LINK C | |
|---|---|---|---|---|---|---|
| | ROLE | WT | ROLE | WT | ROLE | WT |
| Ceramic materials<br>Refractory materials<br>Test methods<br>Brittleness<br>Impact properties<br>Fatigue properties<br>Crack energy properties<br>Biaxial properties<br>Fracture mechanics | | | | | | |

INSTRUCTIONS

1. ORIGINATING ACTIVITY: Enter the name and address of the contractor, subcontractor, grantee, Department of Defense activity or other organization *(corporate author)* issuing the report.

2a. REPORT SECURITY CLASSIFICATION: Enter the overall security classification of the report. Indicate whether "Restricted Data" is included. Marking is to be in accordance with appropriate security regulations.

2b. GROUP: Automatic downgrading is specified in DoD Directive 5200.10 and Armed Forces Industrial Manual. Enter the group number. Also, when applicable, show that optional markings have been used for Group 3 and Group 4 as authorized.

3. REPORT TITLE: Enter the complete report title in all capital letters. Titles in all cases should be unclassified. If a meaningful title cannot be selected without classification, show title classification in all capitals in parenthesis immediately following the title.

4. DESCRIPTIVE NOTES: If appropriate, enter the type of report, e.g., interim, progress, summary, annual, or final. Give the inclusive dates when a specific reporting period is covered.

5. AUTHOR(S): Enter the name(s) of author(s) as shown on or in the report. Enter last name, first name, middle initial. If military, show rank and branch of service. The name of the principal author is an absolute minimum requirement.

6. REPORT DATE: Enter the date of the report as day, month, year, or month, year. If more than one date appears on the report, use date of publication.

7a. TOTAL NUMBER OF PAGES: The total page count should follow normal pagination procedures, i.e., enter the number of pages containing information.

7b. NUMBER OF REFERENCES: Enter the total number of references cited in the report.

8a. CONTRACT OR GRANT NUMBER: If appropriate, enter the applicable number of the contract or grant under which the report was written.

8b, 8c, & 8d. PROJECT NUMBER: Enter the appropriate military department identification, such as project number, subproject number, system numbers, task number, etc.

9a. ORIGINATOR'S REPORT NUMBER(S): Enter the official report number by which the document will be identified and controlled by the originating activity. This number must be unique to this report.

9b. OTHER REPORT NUMBER(S): If the report has been assigned any other report numbers *(either by the originator or by the sponsor)*, also enter this number(s).

10. AVAILABILITY/LIMITATION NOTICES: Enter any limitations on further dissemination of the report, other than those imposed by security classification, using standard statements such as:

(1) "Qualified requesters may obtain copies of this report from DDC."

(2) "Foreign announcement and dissemination of this report by DDC is not authorized."

(3) "U. S. Government agencies may obtain copies of this report directly from DDC. Other qualified DDC users shall request through _____."

(4) "U. S. military agencies may obtain copies of this report directly from DDC. Other qualified users shall request through _____."

(5) "All distribution of this report is controlled. Qualified DDC users shall request through _____."

If the report has been furnished to the Office of Technical Services, Department of Commerce, for sale to the public, indicate this fact and enter the price, if known.

11. SUPPLEMENTARY NOTES: Use for additional explanatory notes.

12. SPONSORING MILITARY ACTIVITY: Enter the name of the departmental project office or laboratory sponsoring *(paying for)* the research and development. Include address.

13. ABSTRACT: Enter an abstract giving a brief and factual summary of the document indicative of the report, even though it may also appear elsewhere in the body of the technical report. If additional space is required, a continuation sheet shall be attached.

It is highly desirable that the abstract of classified reports be unclassified. Each paragraph of the abstract shall end with an indication of the military security classification of the information in the paragraph, represented as *(TS), (S), (C), or (U)*.

There is no limitation on the length of the abstract. However, the suggested length is from 150 to 225 words.

14. KEY WORDS: Key words are technically meaningful terms or short phrases that characterize a report and may be used as index entries for cataloging the report. Key words must be selected so that no security classification is required. Identifiers, such as equipment model designation, trade name, military project code name, geographic location, may be used as key words but will be followed by an indication of technical context. The assignment of links, rules, and weights is optional.